The compact FFGS (or CFFGIVUVS)

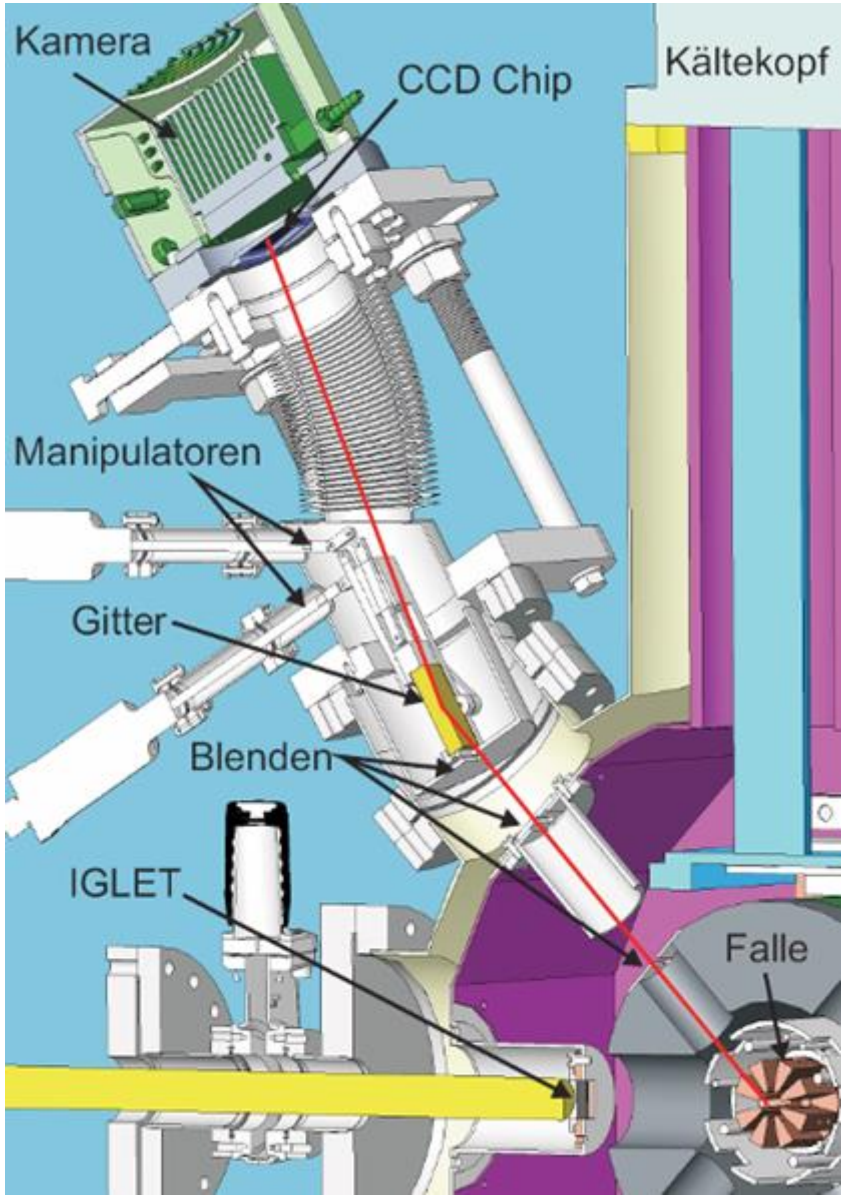

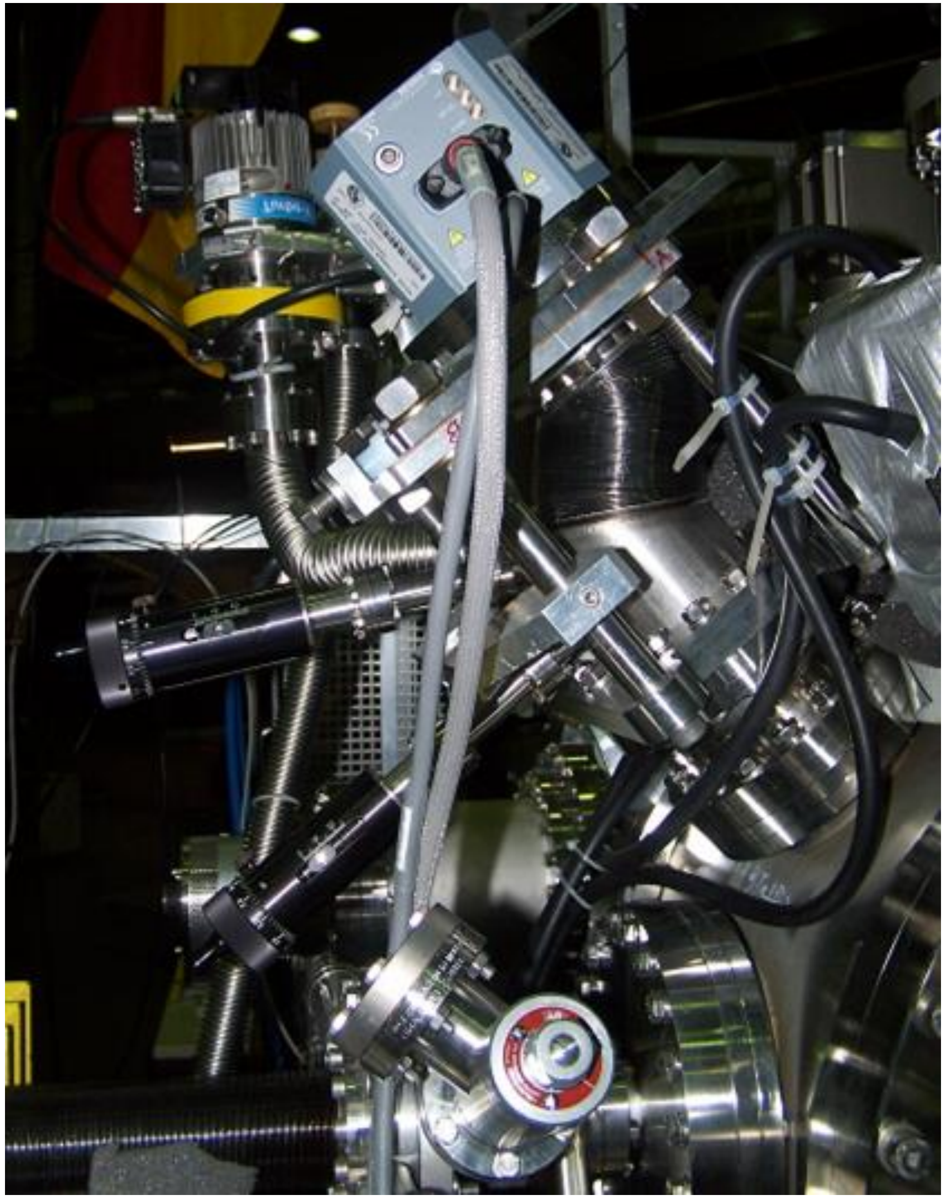

Spectral image (untreated)

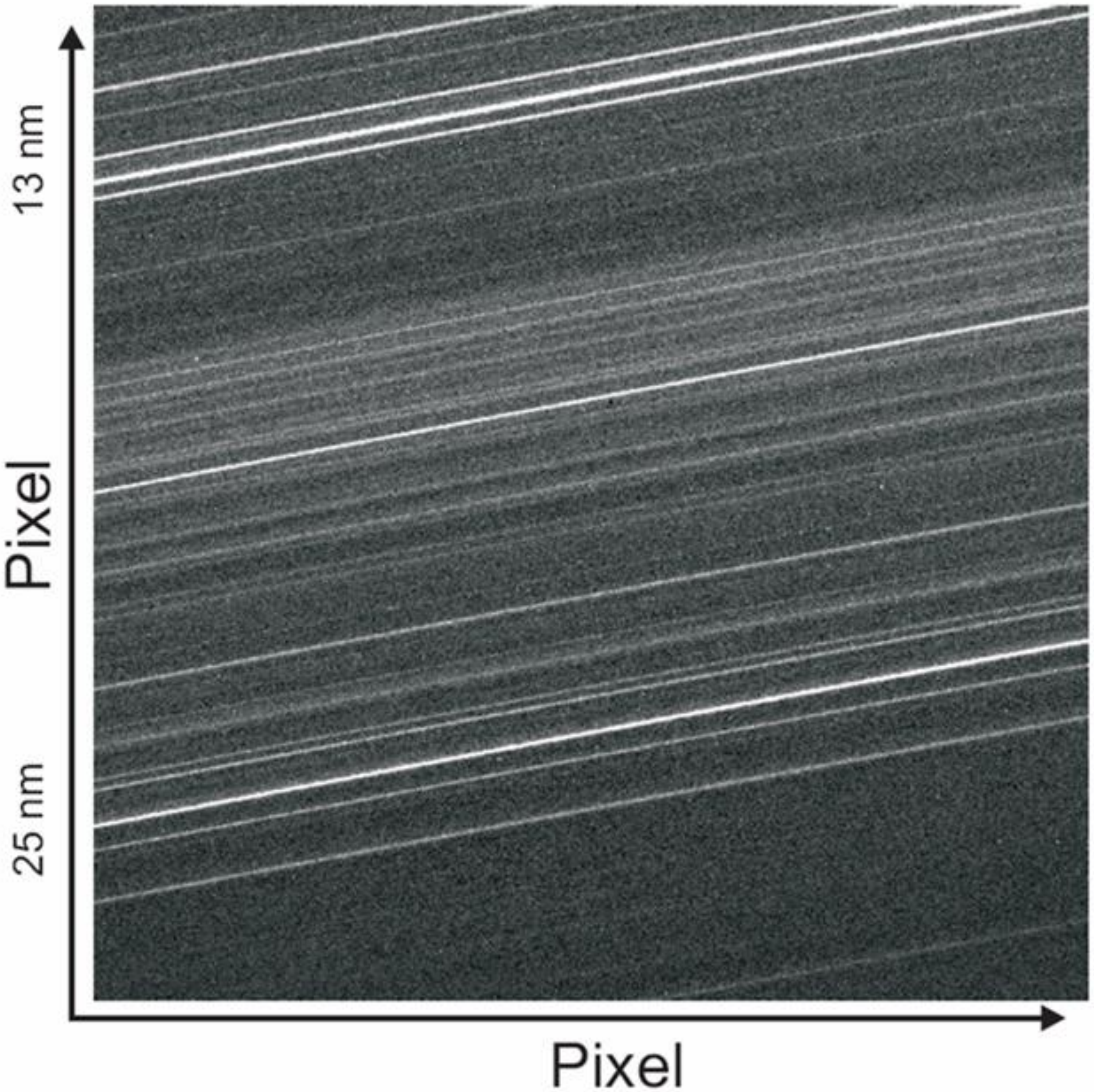

CCD spectral image

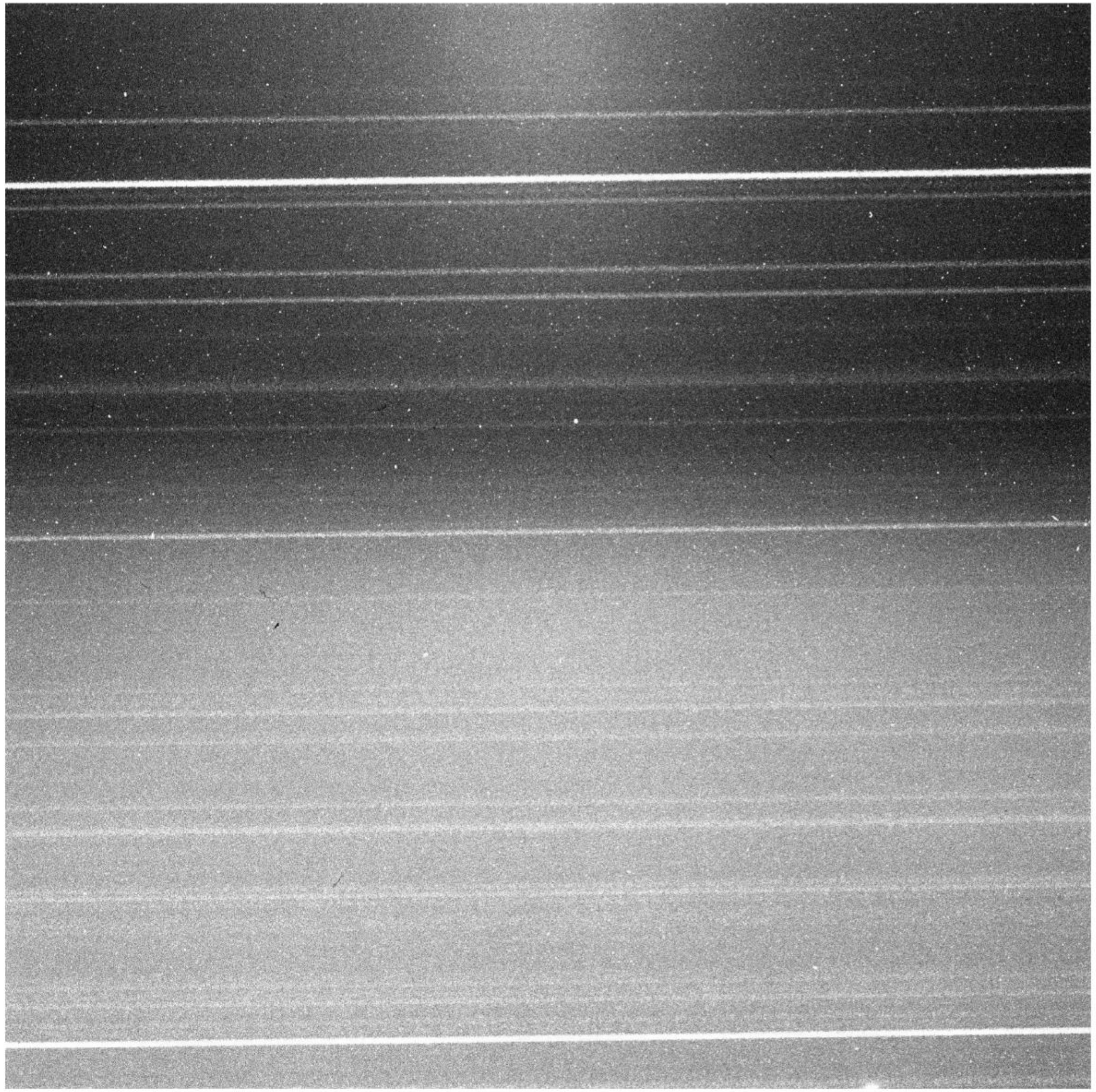

Resolving power

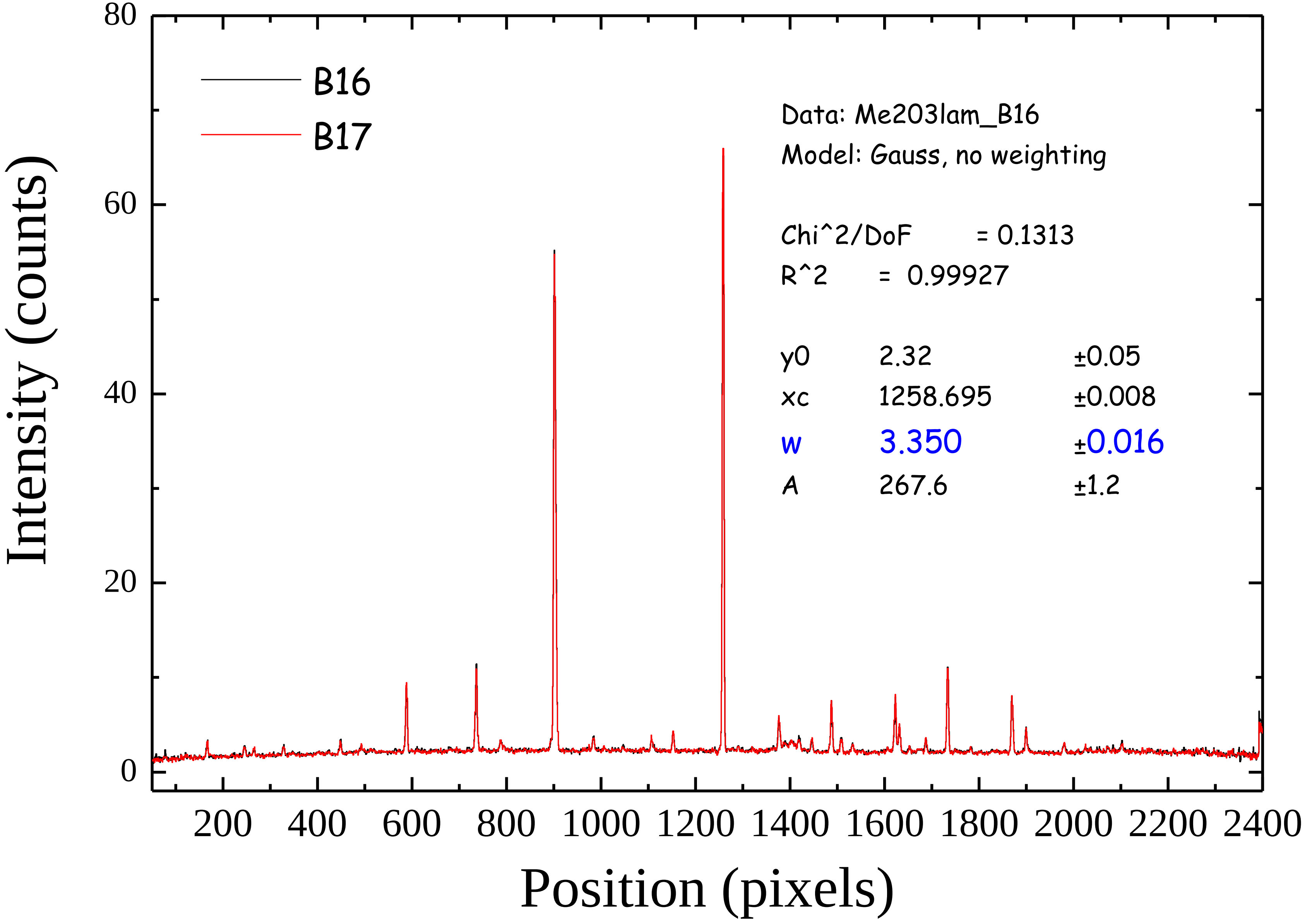

Calibration lines of O and N

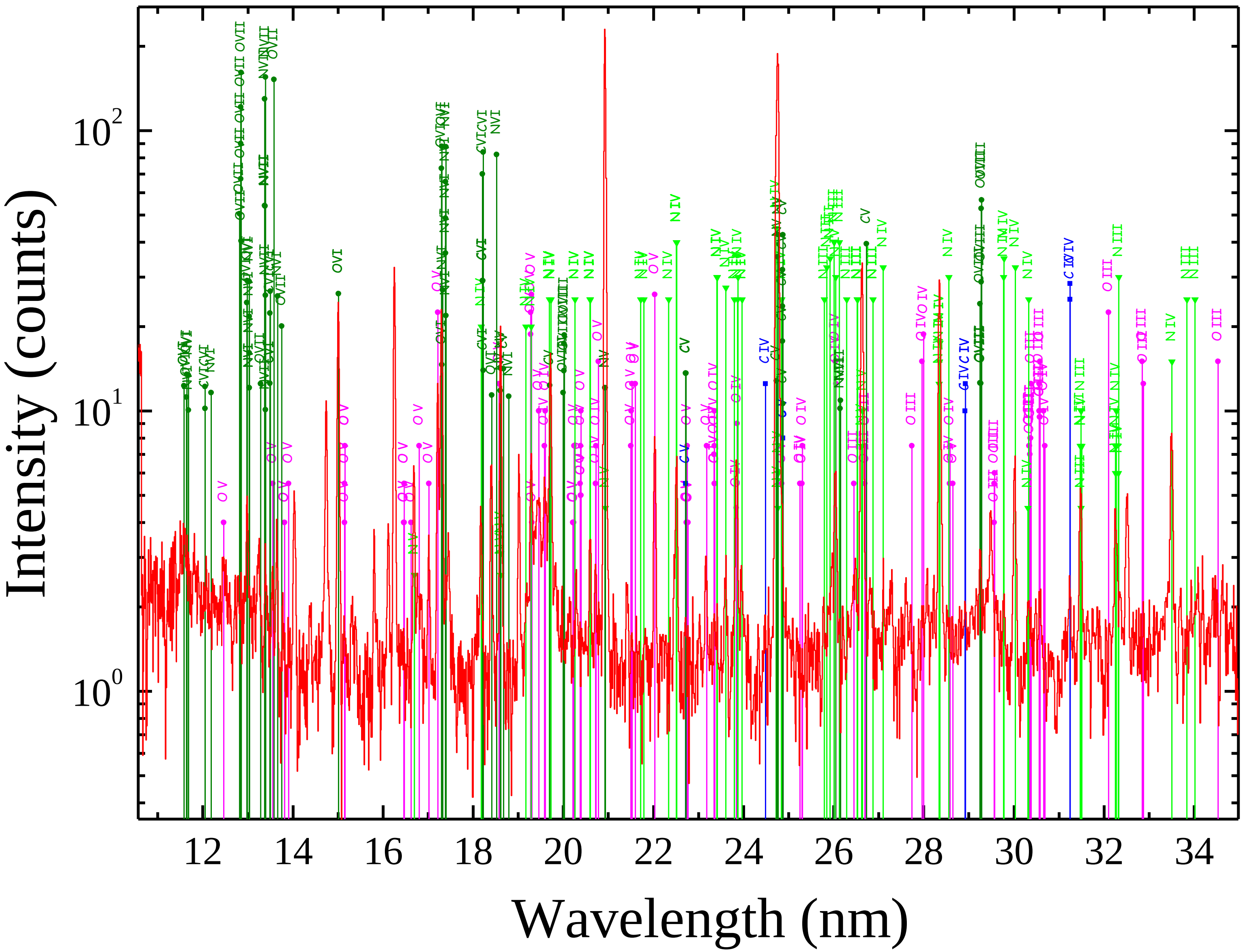

Spectral simulations with CHIANTI compared with data

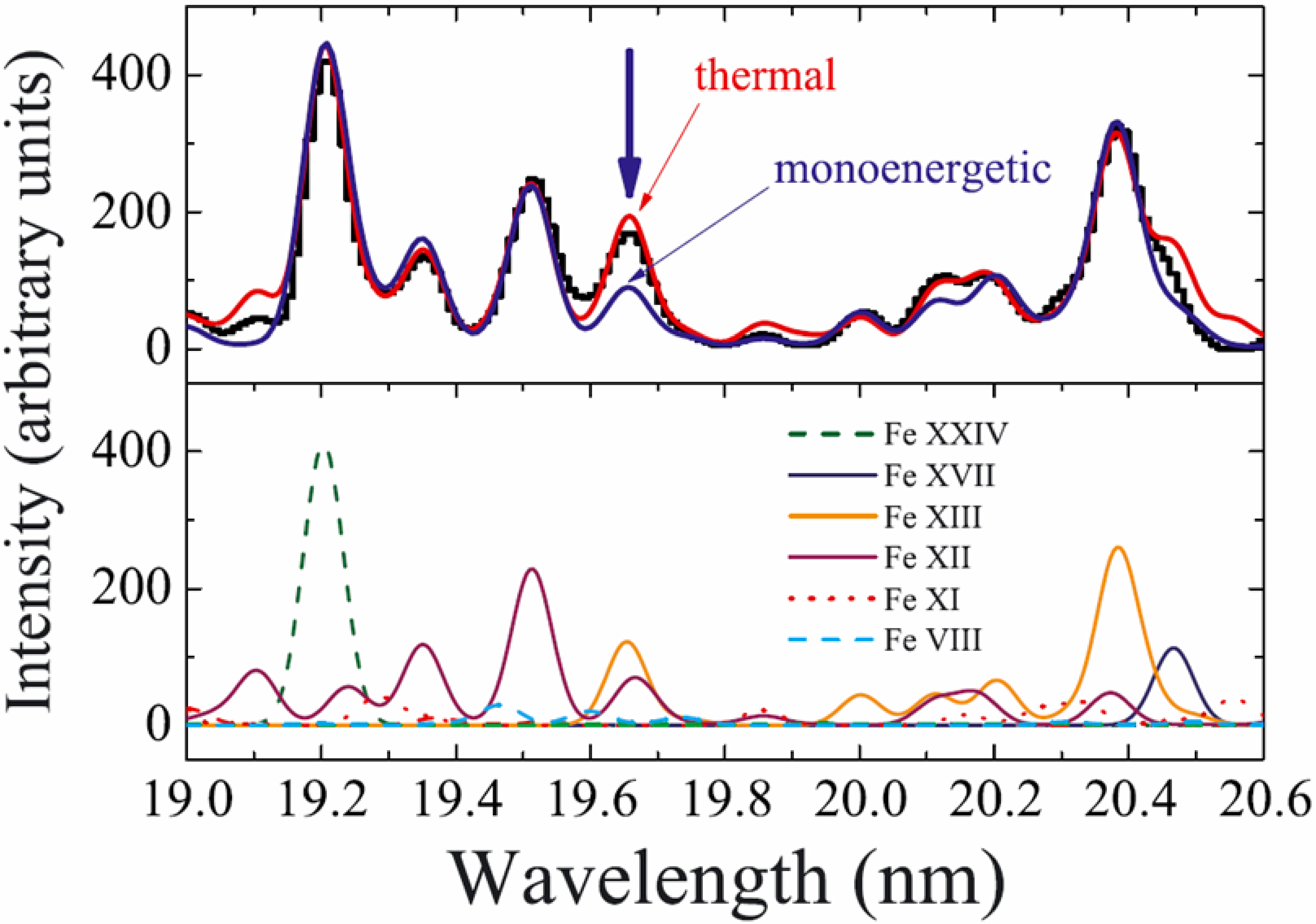

VUV spectra energy dependence

The spectra are monitored as the electron beam energy is varied in steps of 3 eV shown together in a composite image.

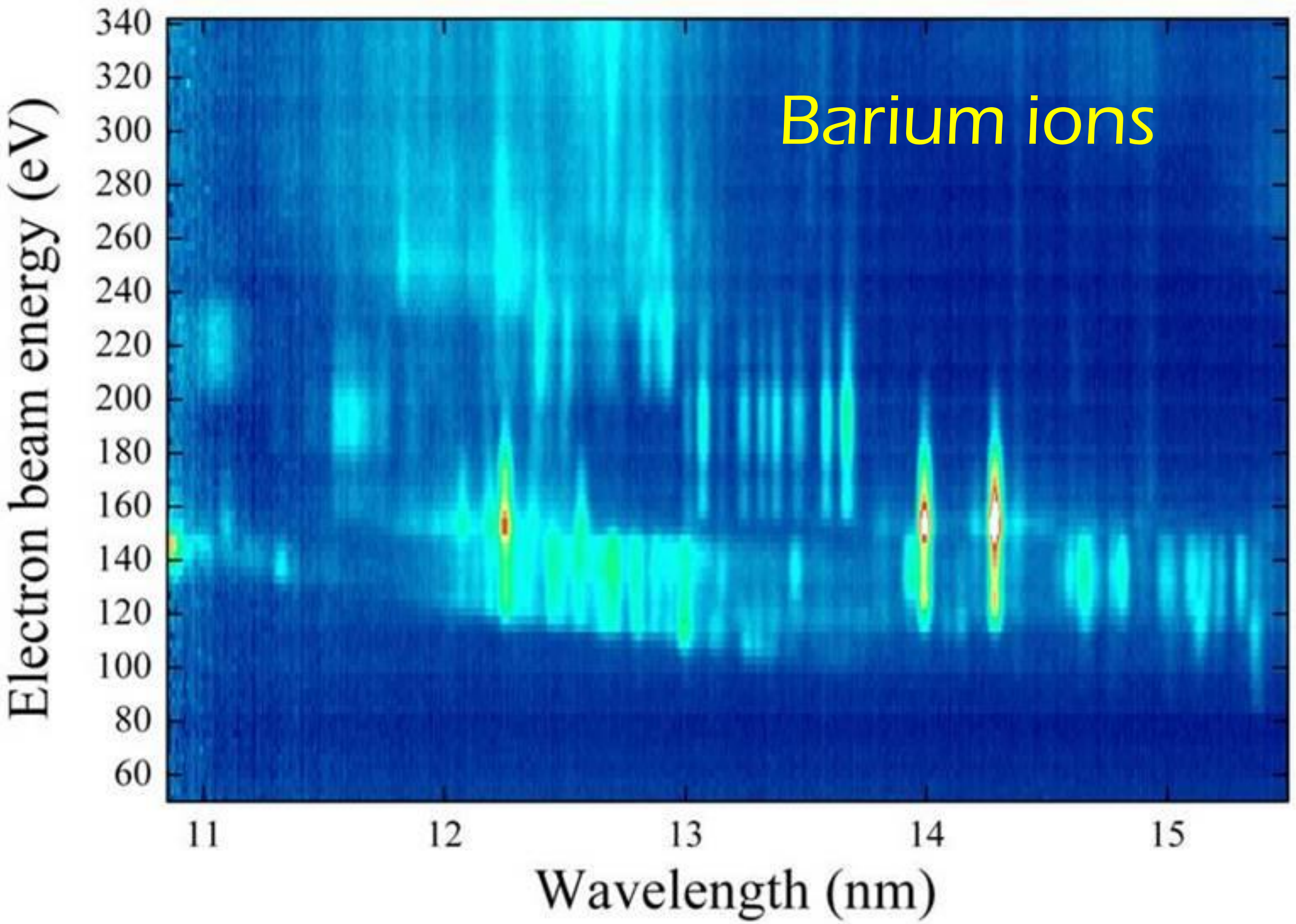

Xenon for microlithography

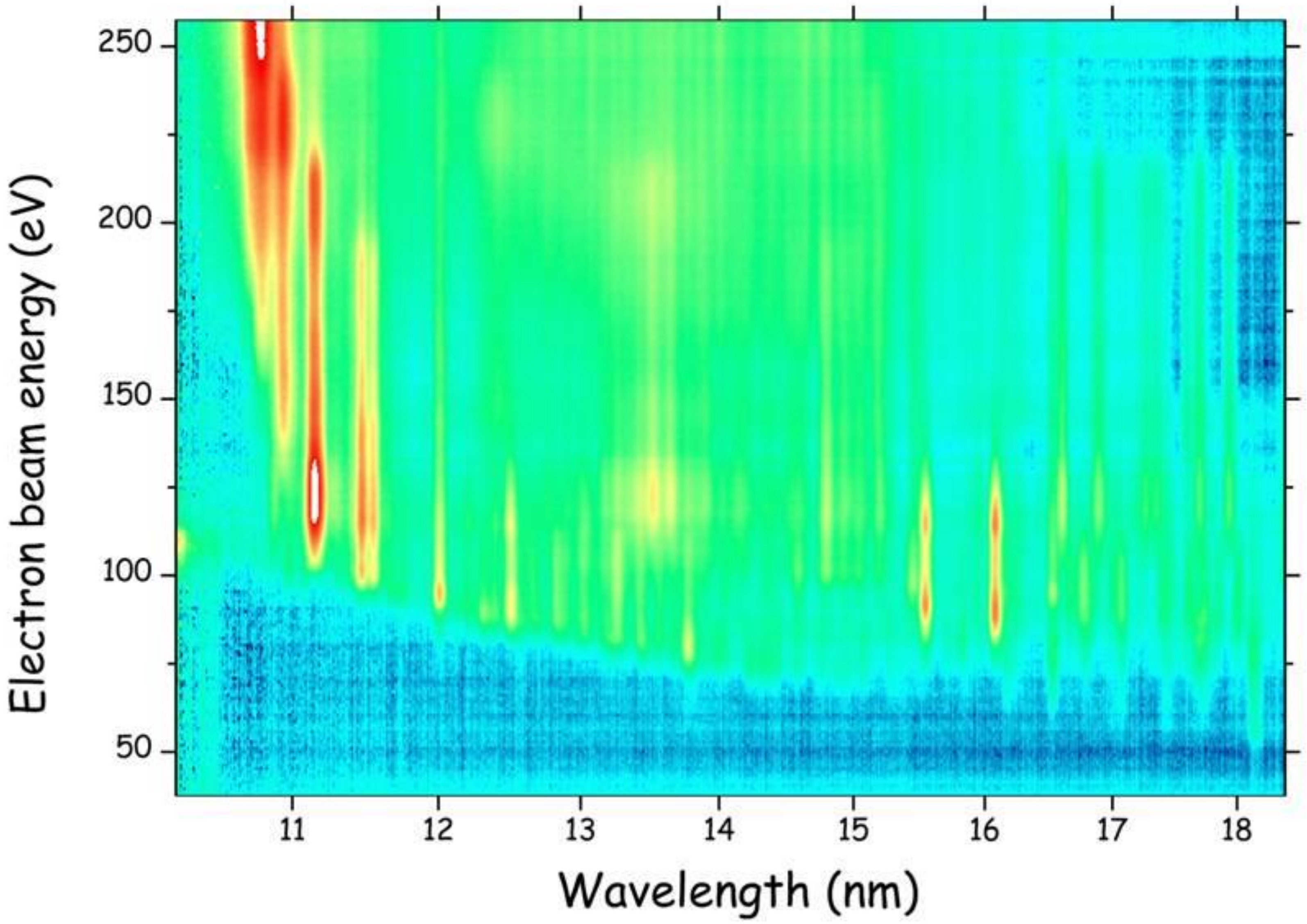

Excitation energy dependency

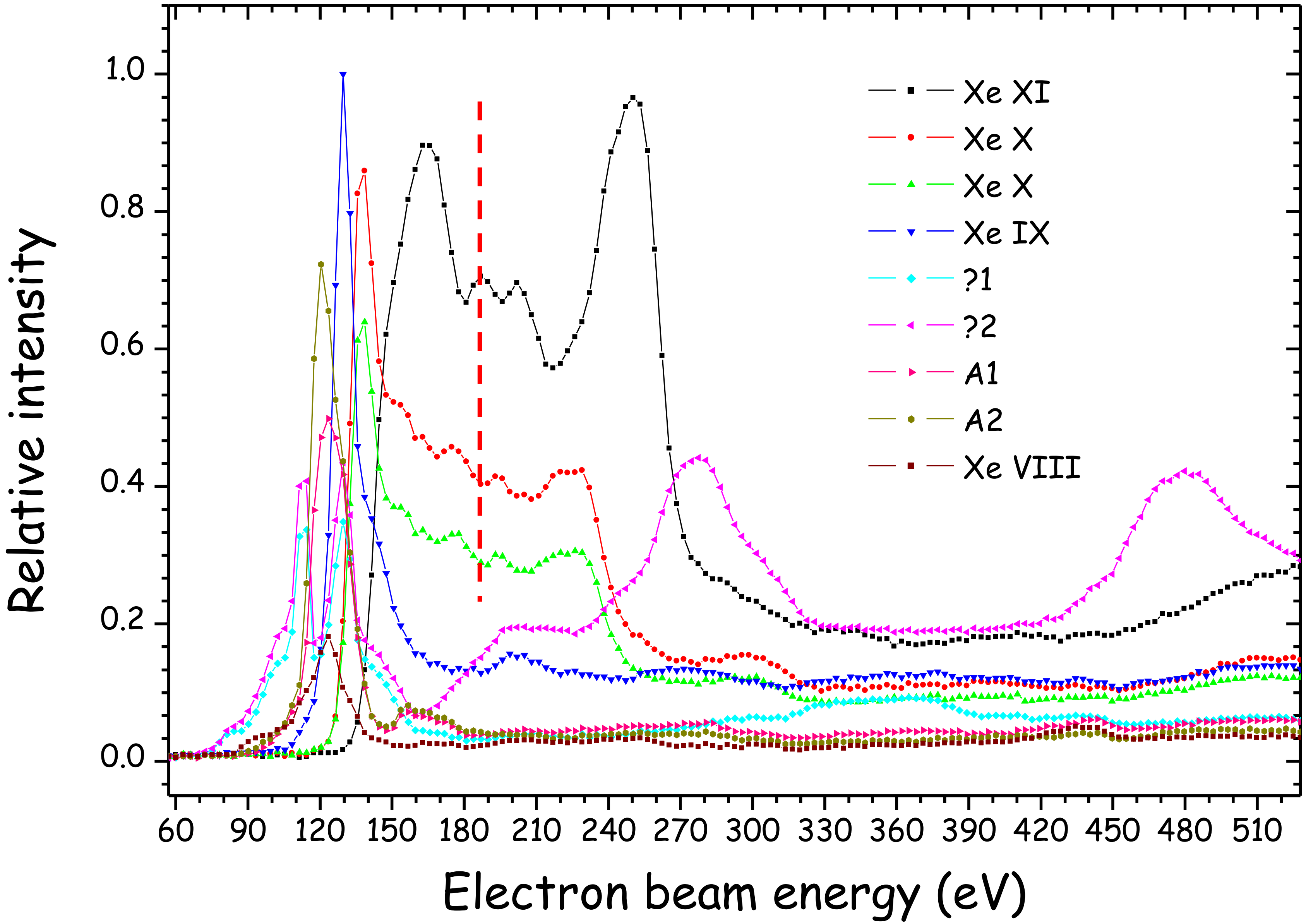

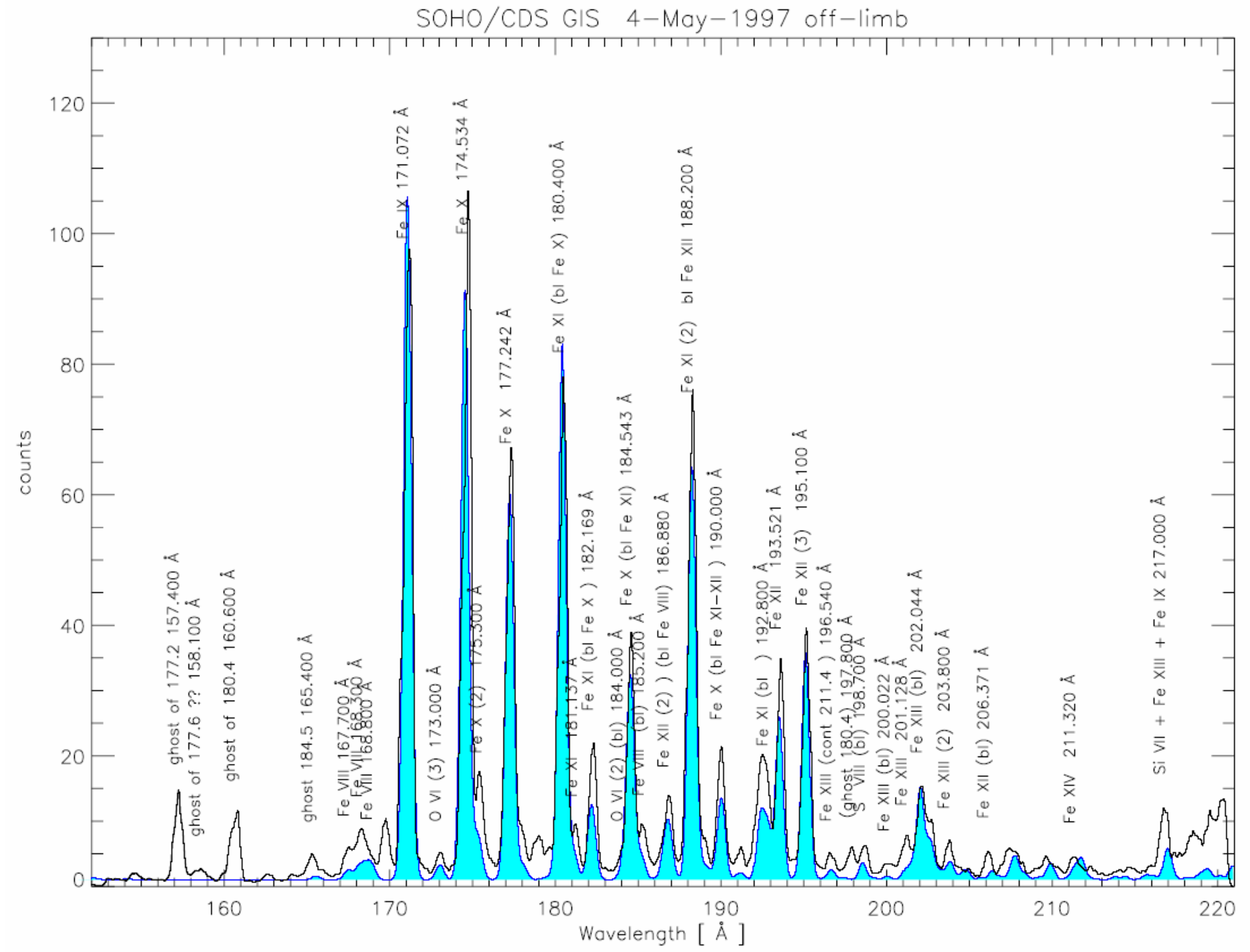

GIS 1 spectrum of an off-limb quiet sun observation (May 4th 1997), with corresponding synthetic spectra overlaid. These types of spectra have been mainly used for the first order internal and cross-detector calibration.

G. Del Zanna, B. J. I. Bromage, E. Landi, and M. Landini, A&A 379, 708 (2001)

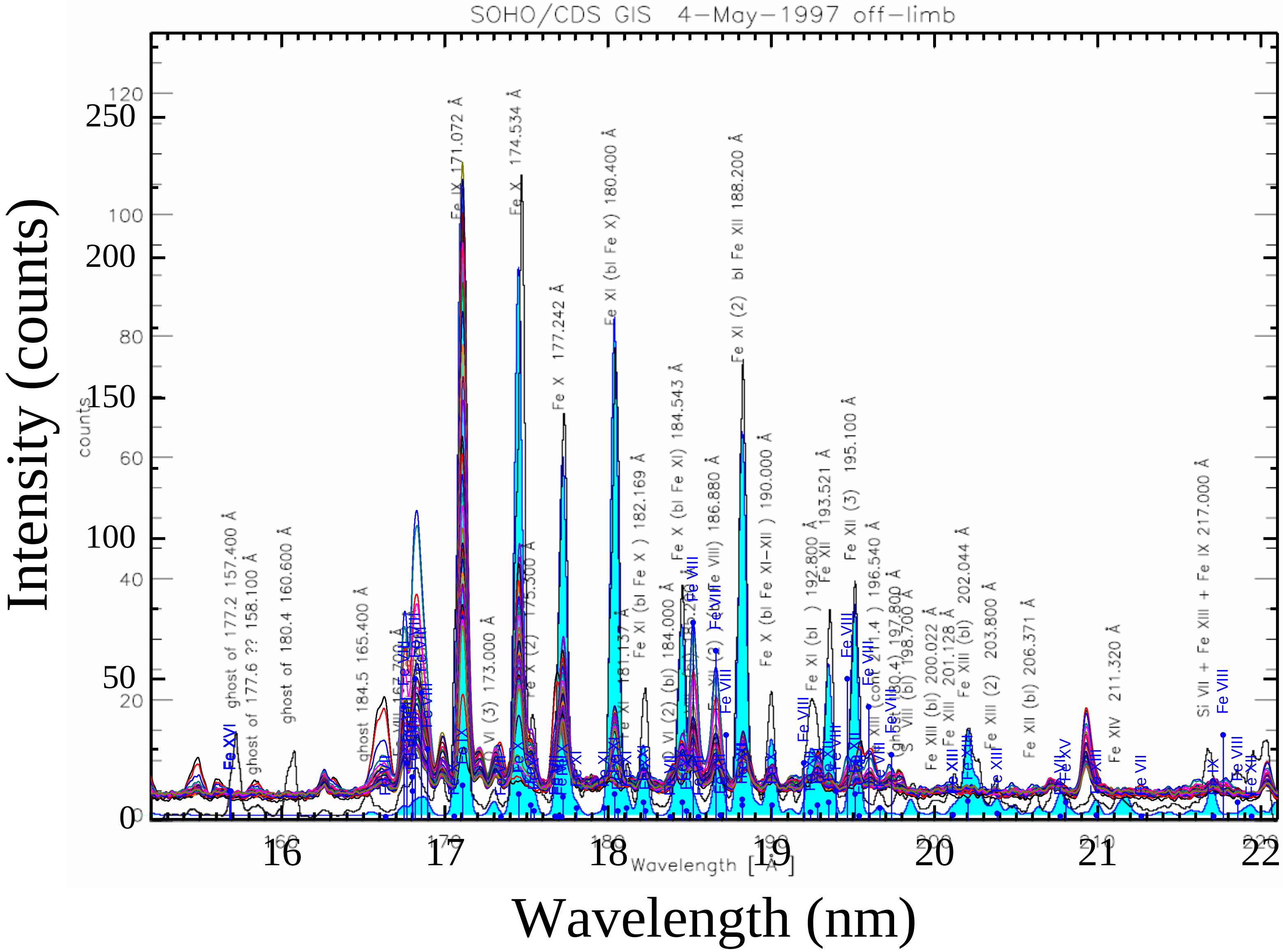
SOHO/CDS GIS 4-May-1997 off-limb
Intensity (counts)
Wavelength (nm)
Wavelength [Å]
counts
Fe IX 171.072 Å
Fe X 174.534 Å
Fe X 177.242 Å
Fe XI (bl Fe X) 180.400 Å
Fe XI (2) bl Fe XII 188.200 Å
Fe X (bl Fe XI) 184.543 Å
Fe XI (bl Fe X) 182.169 Å
Fe X (bl Fe XI–XII) 190.000 Å
Fe XII (3) 195.100 Å
Fe XII 193.521 Å
Fe XIII (bl) 202.044 Å
Fe XIII (2) 203.800 Å
Fe XII (bl) 206.371 Å
Fe XIV 211.320 Å
Si VII + Fe XIII + Fe IX 217.000 Å
ghost of 177.2 157.400 Å
ghost of 177.6 ?? 158.100 Å
ghost of 180.4 160.600 Å
ghost 184.5 165.400 Å
Fe XVI
Fe VIII
Fe XV
Fe VII

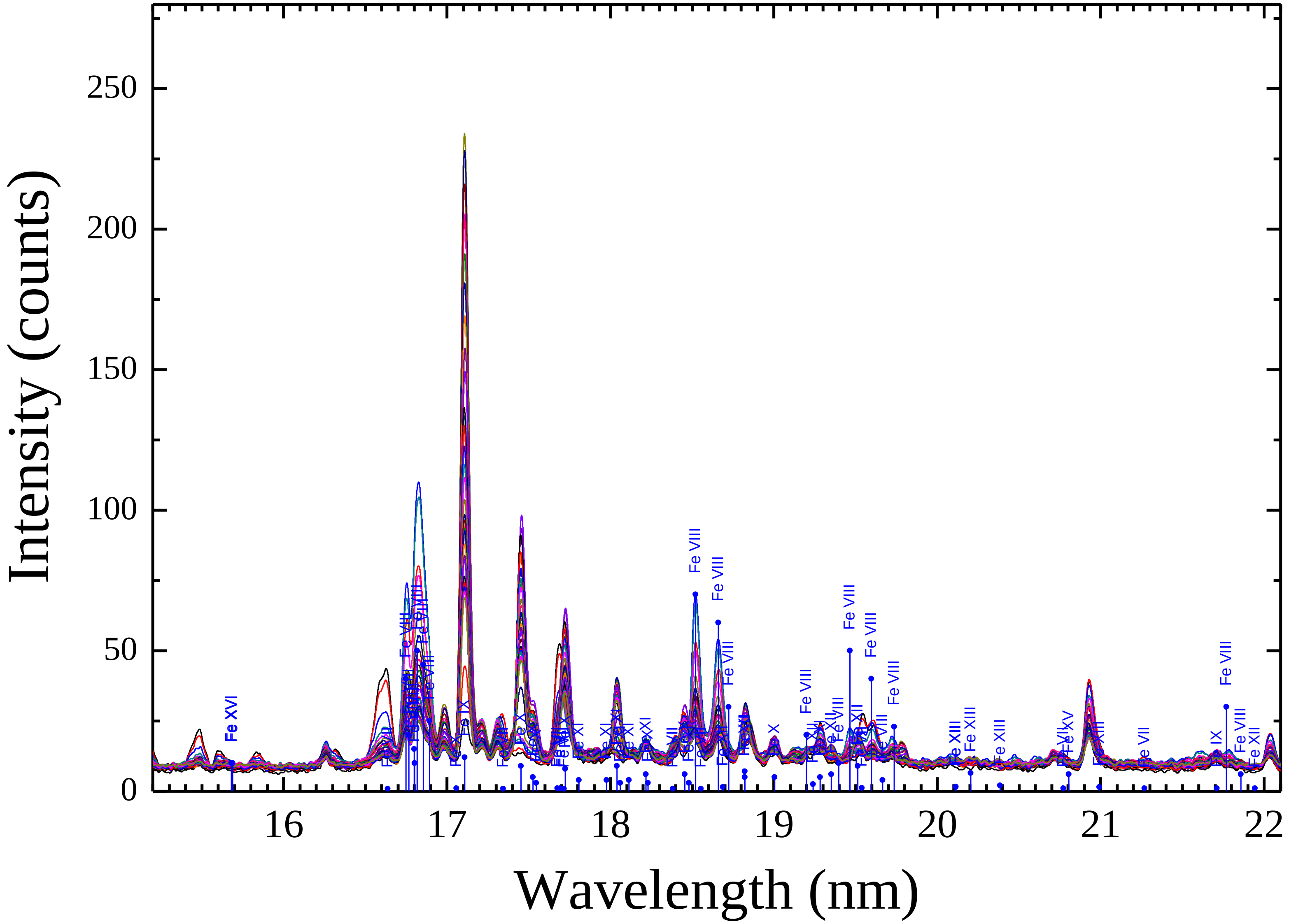
Intensity (counts)
Wavelength (nm)
0
50
100
150
200
250
16
17
18
19
20
21
22
Fe XVI
Fe VIII
Fe VIII
Fe VIII
Fe VIII
Fe VIII
Fe VIII
Fe VIII
Fe VIII
Fe VIII
Fe XIII
Fe XIII
Fe XIII
Fe XV
Fe VII
Fe VIII
Fe XII

Comparison

of new data

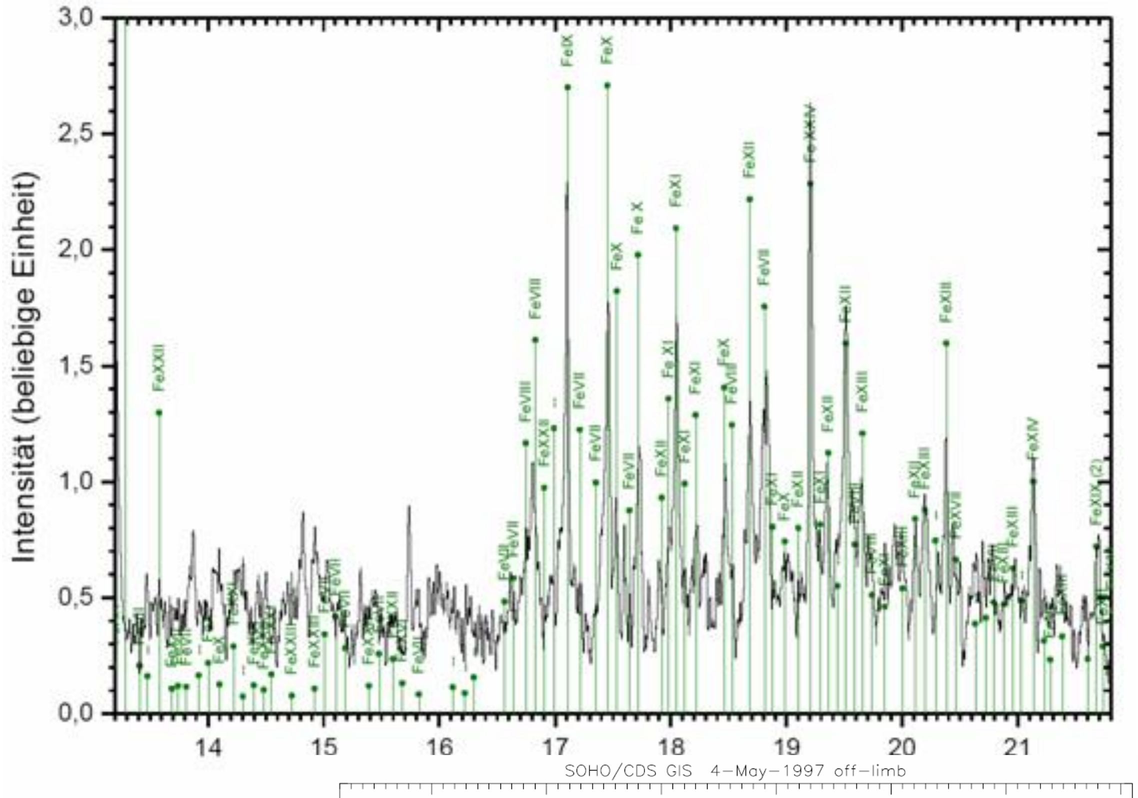

with

SOHO

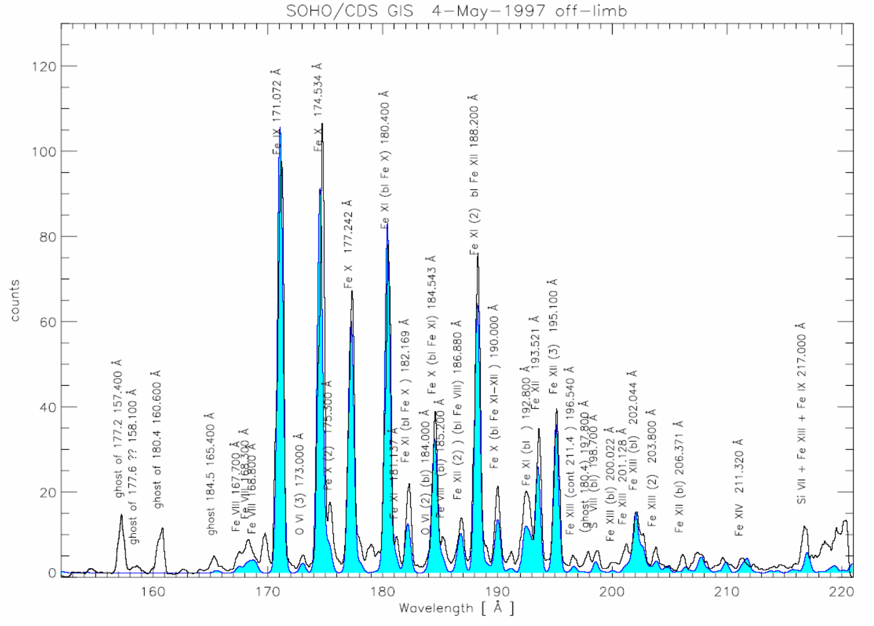

The new flat field grating spectrometer (Baumann 2008)

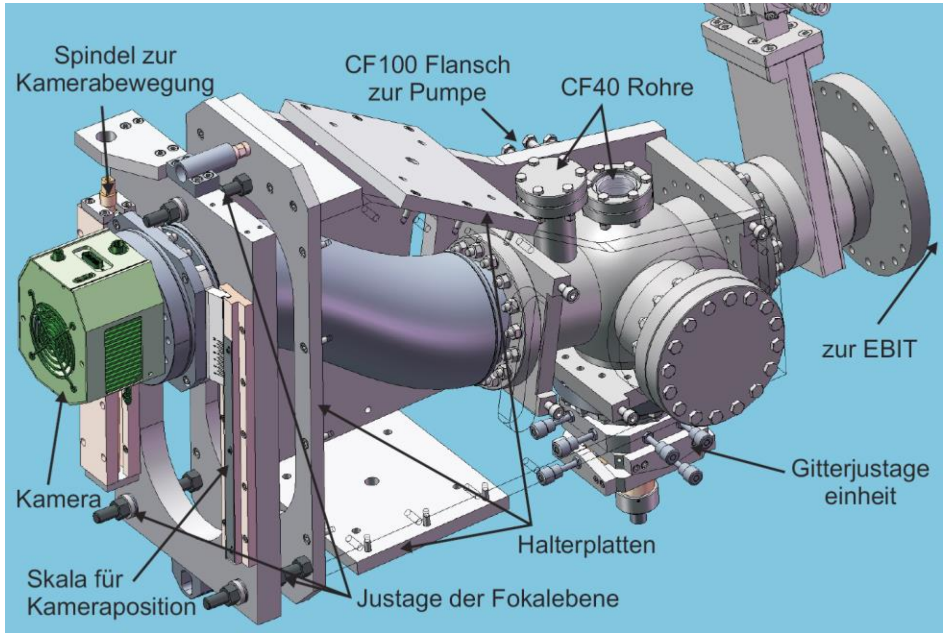

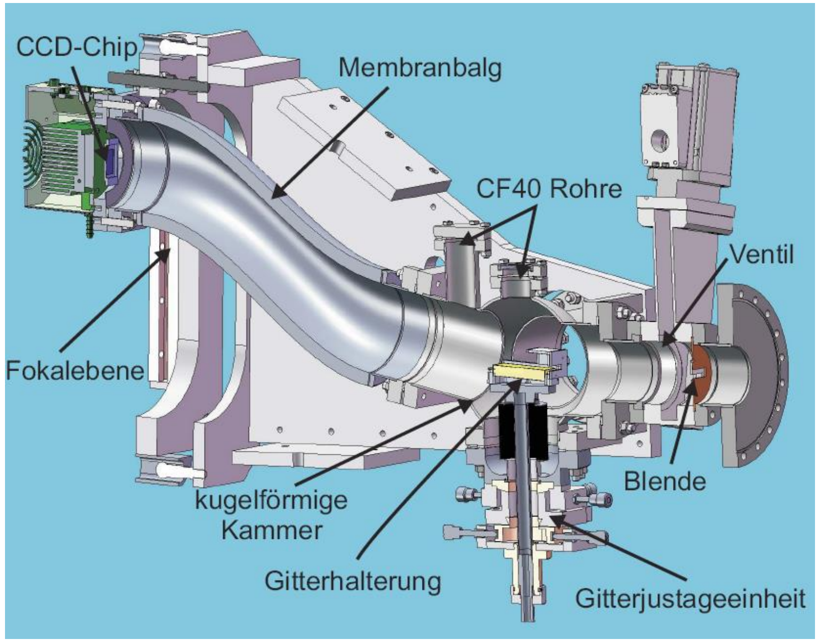

Diploma thesis Thomas Baumann:
- Hitachi gratings
- Range 25-200 eV
- Resolving power 1500
- CCD at -95°C, 2048x2048 pixels

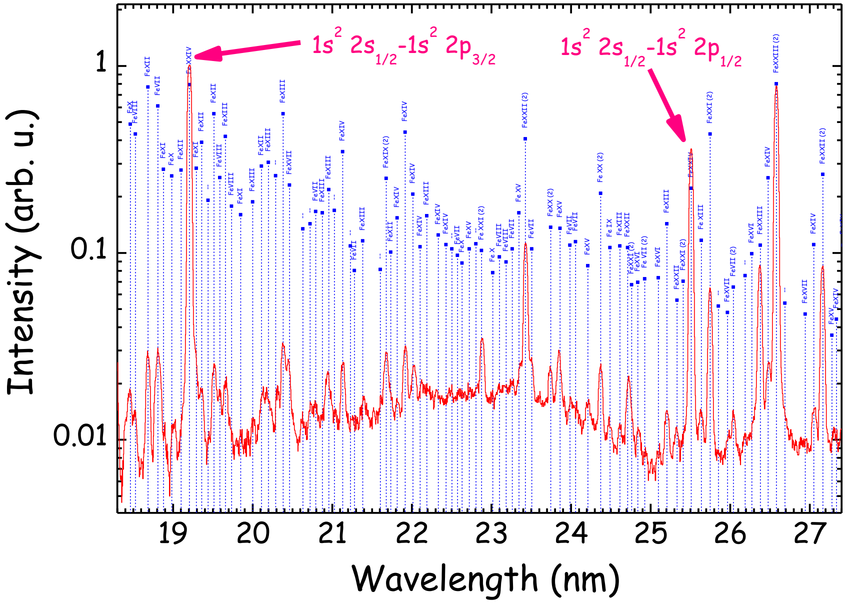

The new flat field grating spectrometer (Baumann 2008)

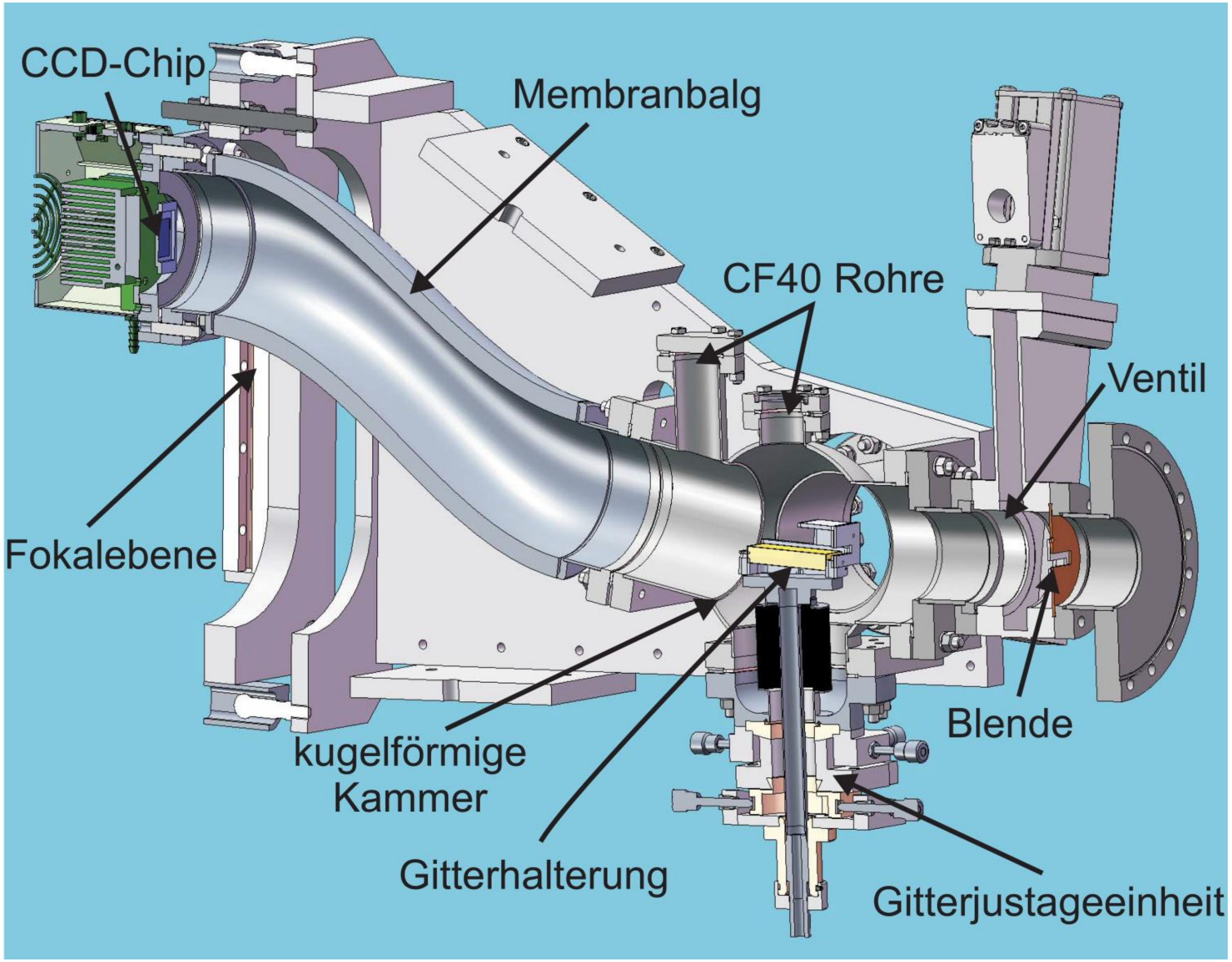

The new flat field grating spectrometer (Baumann 2008)

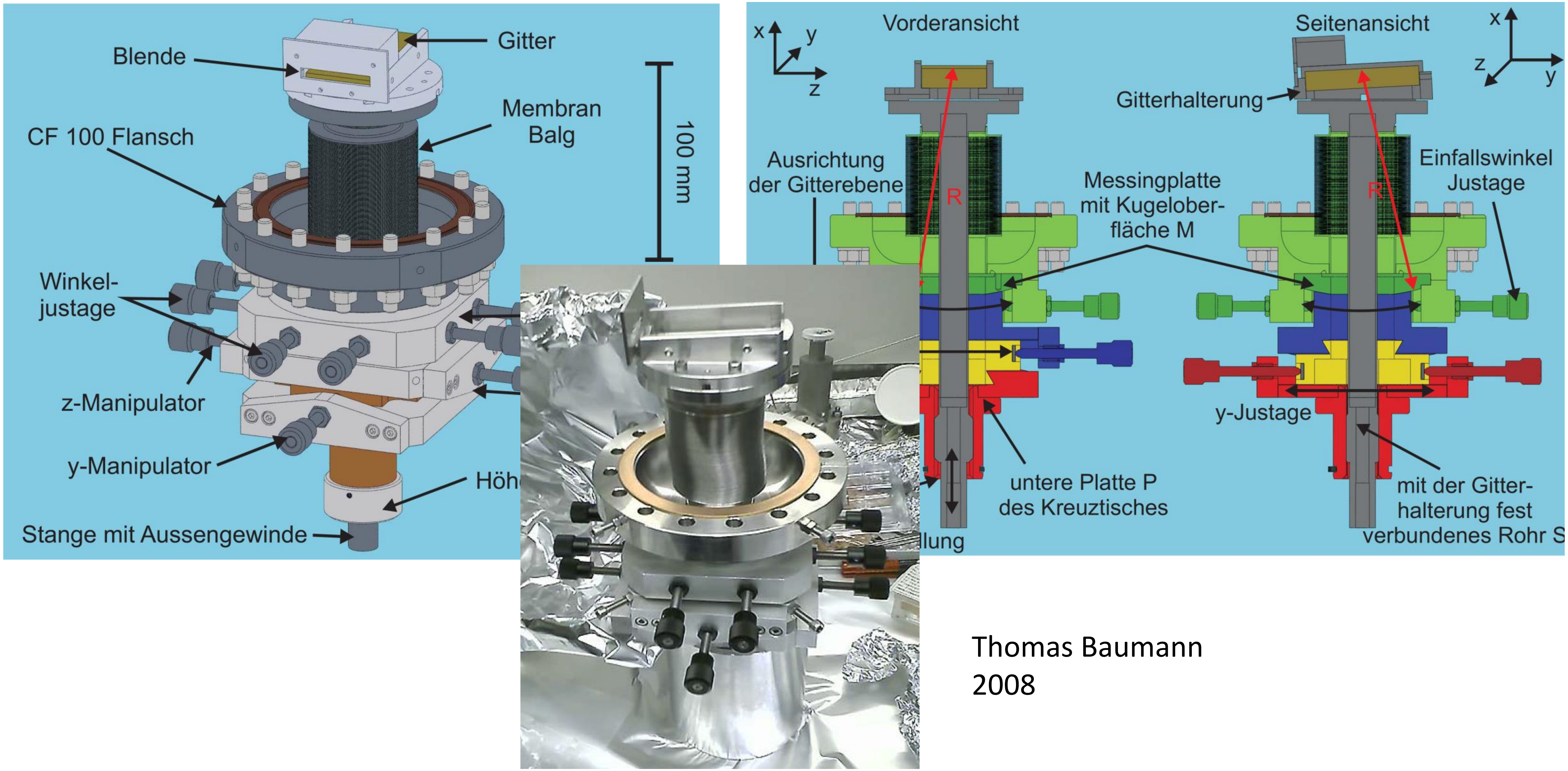

Thomas Baumann
2008

Focal plane of flat field grating spectrometer (Baumann 2008)

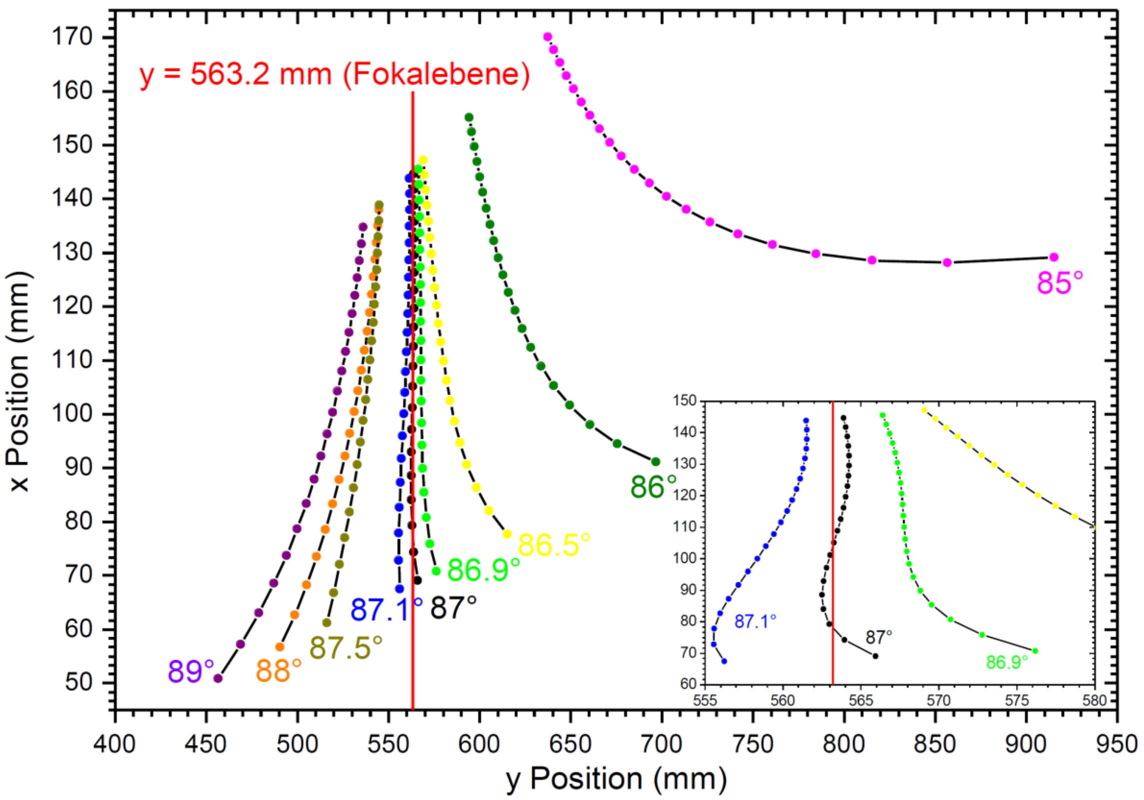

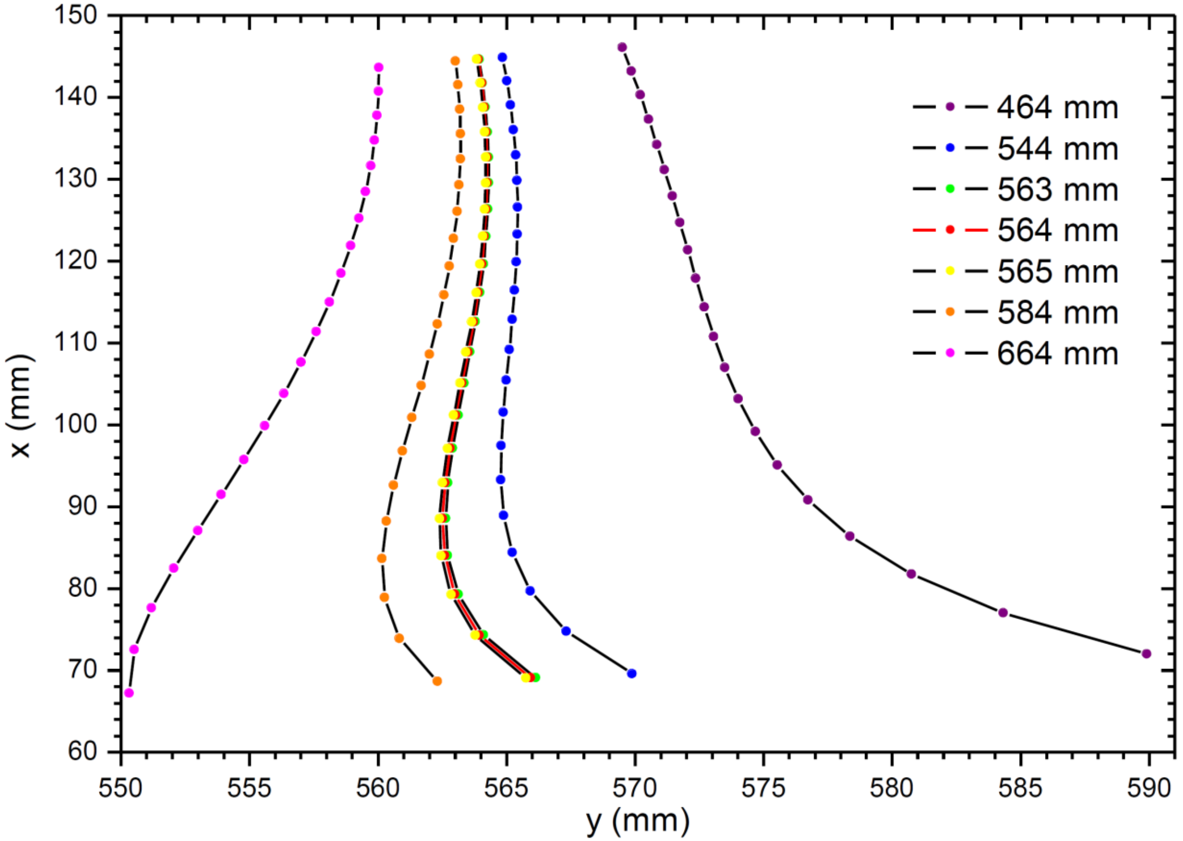

Horizontale Fokalkurven von Gitter II für unterschiedliche Einfallswinkel . Der kleine Graph zeigt den vergrößerten Bereich um 87 grad

Fokalkurven von Gitter II für unterschiedliche Quellendistanzen r

Selectivity of charge states with electron beam energy

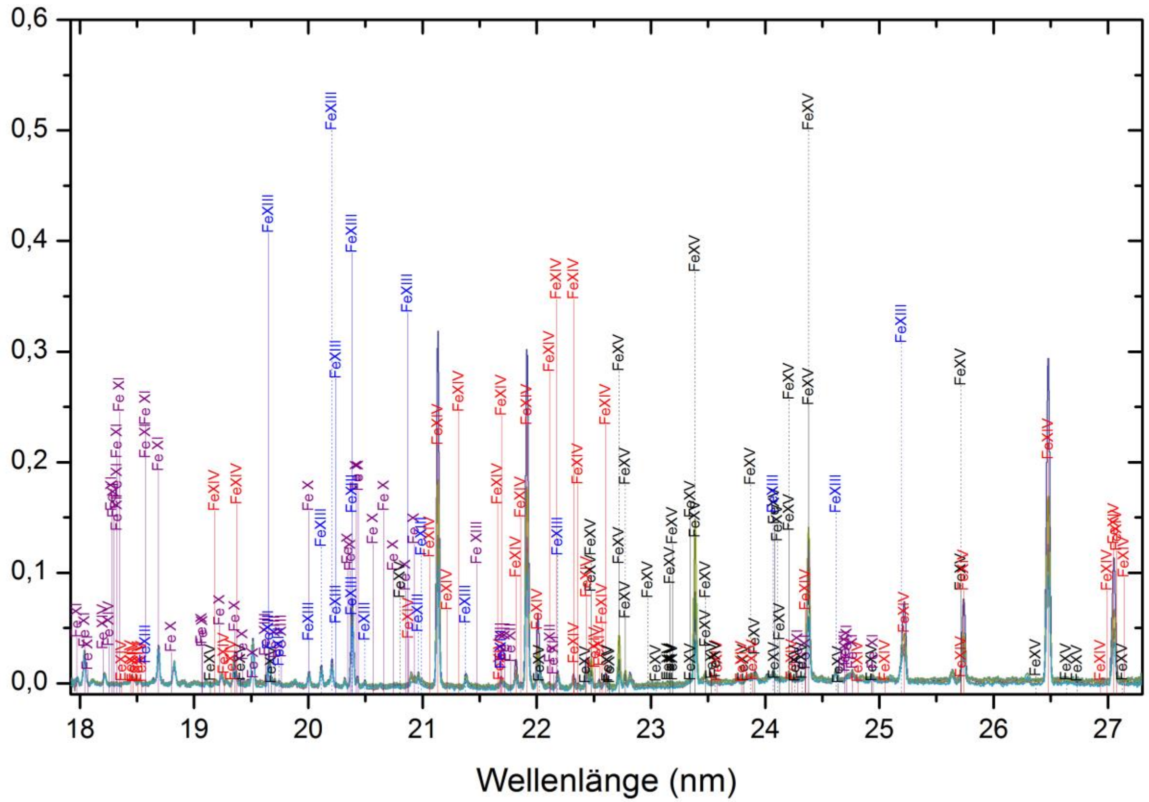

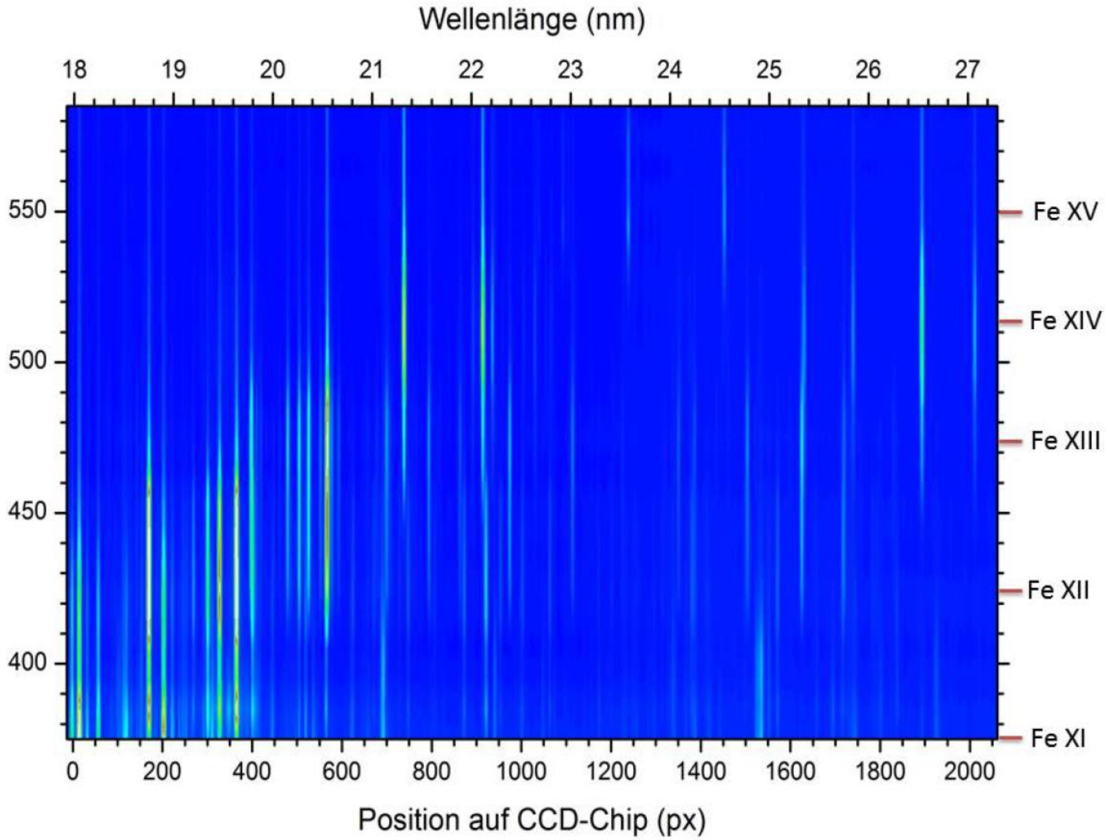

Selectivity of charge states with electron beam energy

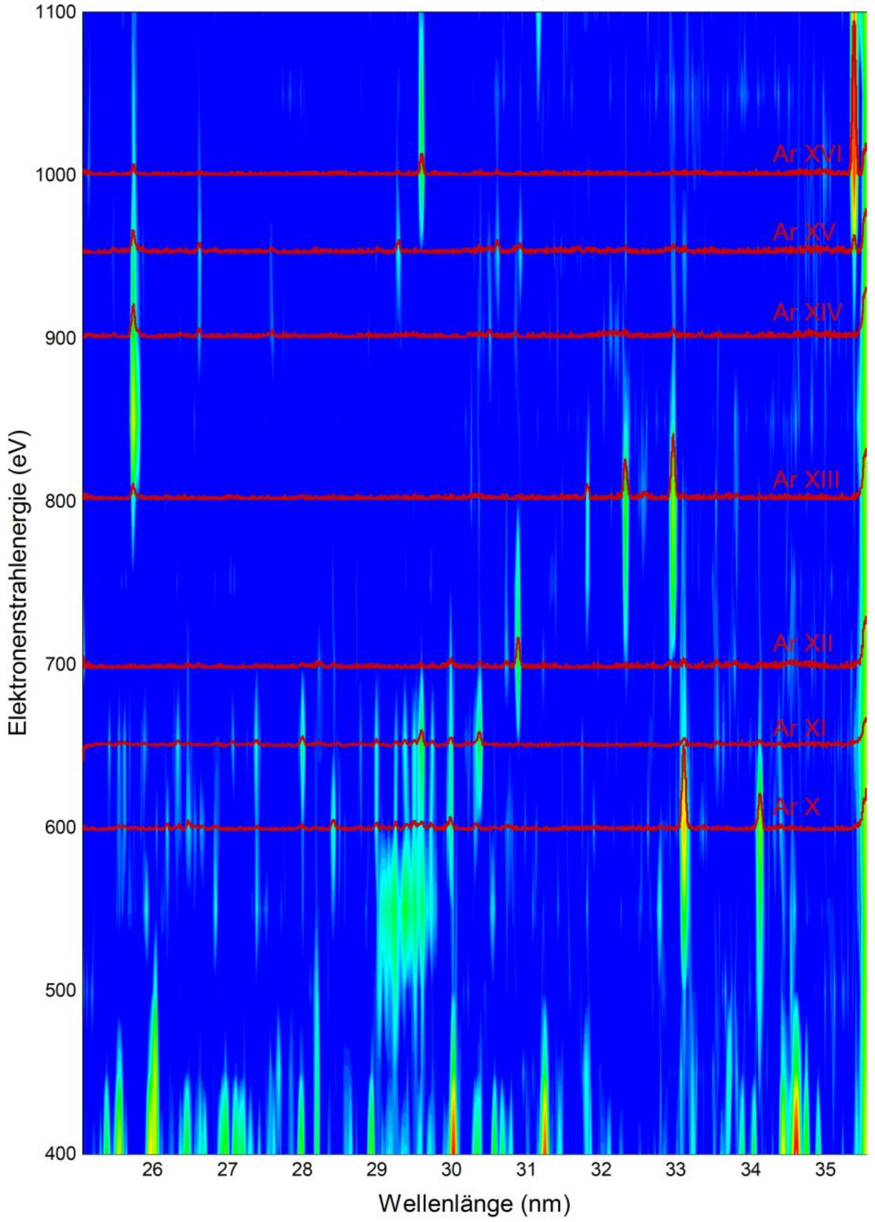

Reproducibility and error bars in the XUV

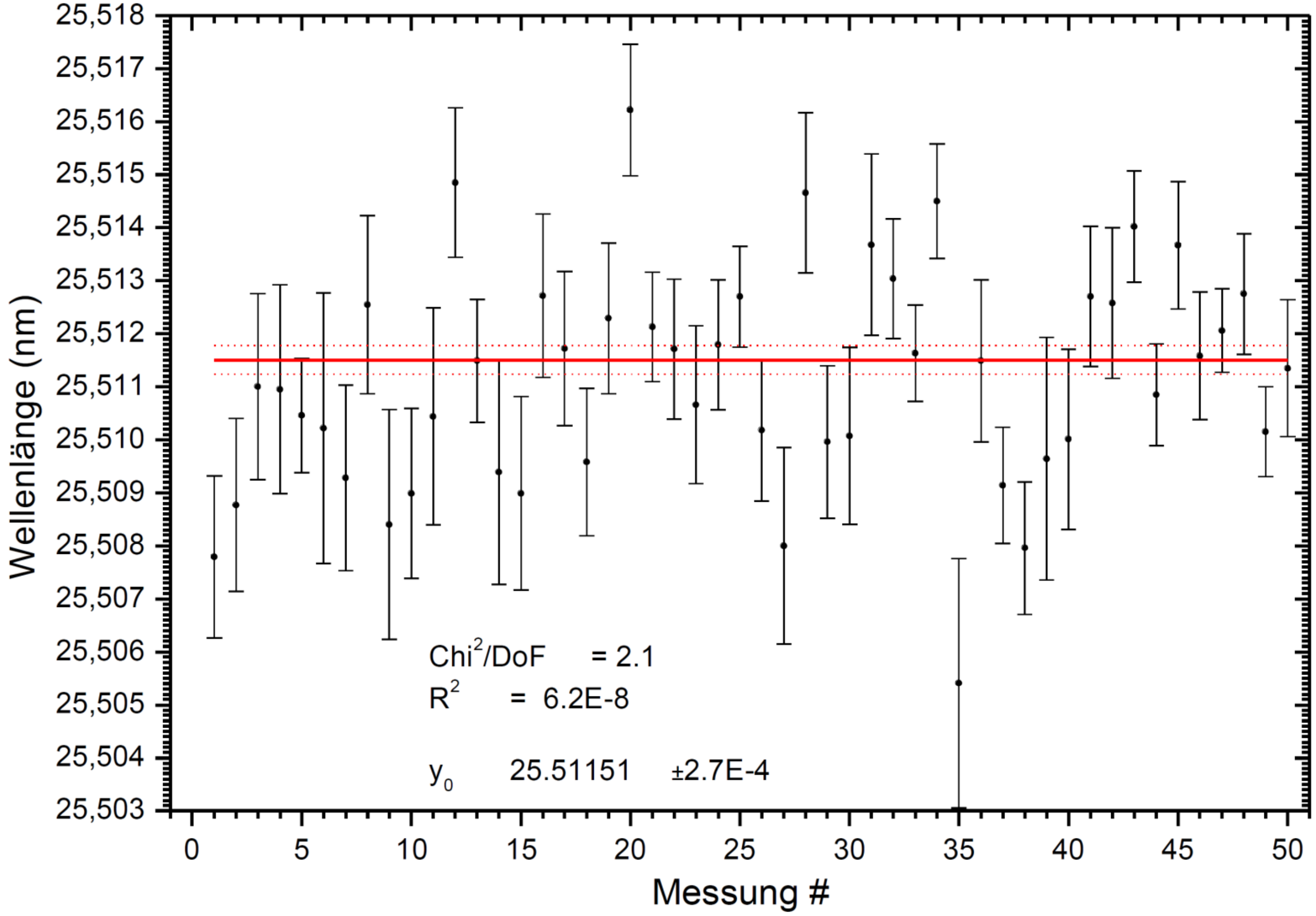

Abbildung 5.14: Wellenlänge des $1s^2 2s\, S_{1/2} - 1s^2 2p\, P_{3/2}$ Übergangs in Fe XXIV aller 50 Messungen zusammen mit ihrem statistisch gewichteten Mittelwert und dessen 68% Vertrauensintervall.

Reproducibility and error bars in the XUV

Referenz	Wellenlänge λ (nm)	Fehler $\Delta\lambda$ (nm)	Methode
K. Dere 1978 [41]	19.203	0.003	Sonneneruption
E. Hinnov 1979 [42]	19.205	0.003	Tokamak
E. Hinnov 1989 *et al.* [43]	19.201	0.002	Tokamak
R. J. Knize 1991 [44]	19.2046	0.0009	Tokamak
J. Reader 1994 *et al.* [37]	19.2028	0.0005	Tokamak
S. W. Epp 2007 [10]	19.2017	0.0012	EBIT
S. A. Blundell 1993 [45]	19.2021		Theorie
M. H. Chen 1995 [46]	19.205		Theorie
diese Arbeit	**19.2037**	**0.001**	**EBIT**
K. P. Dere 1978 [41]	25.511	0.003	Sonneneruption
E. Hinnov 1979 [42]	25.511	0.003	Tokamak
E. Hinnov 1989 *et al.* [43]	25.509	0.001	Tokamak
R. J. Knize 1991 [44]	25.511	0.001	Tokamak
J. Reader 1994 *et al.* [37]	25.5113	0.0005	Tokamak
S. W. Epp 2007 [10]	25.5118	0.0002	EBIT
S. A. Blundell 1993 [45]	25.5101		Theorie
M. H. Chen 1995 [46]	25.5111		Theorie
diese Arbeit	**25.5115**	**0.0007**	**EBIT**

Tabelle 5.4: Literaturwerte der beiden Fe XXIV Linien. Zur Messung dieser Linien wurden unterschiedliche Methoden angewandt: Spektrale Untersuchungen von Sonneneruptionen, Spektroskopie an Tokamak Plasmen, Spektroskopie an EBIT Plasmen und theoretische Berechnungen.

Hinode ("sunrise") is a solar space telescope mission launched in 2006 (Japan with US and UK partners) aiming at investigating the Sun's corona

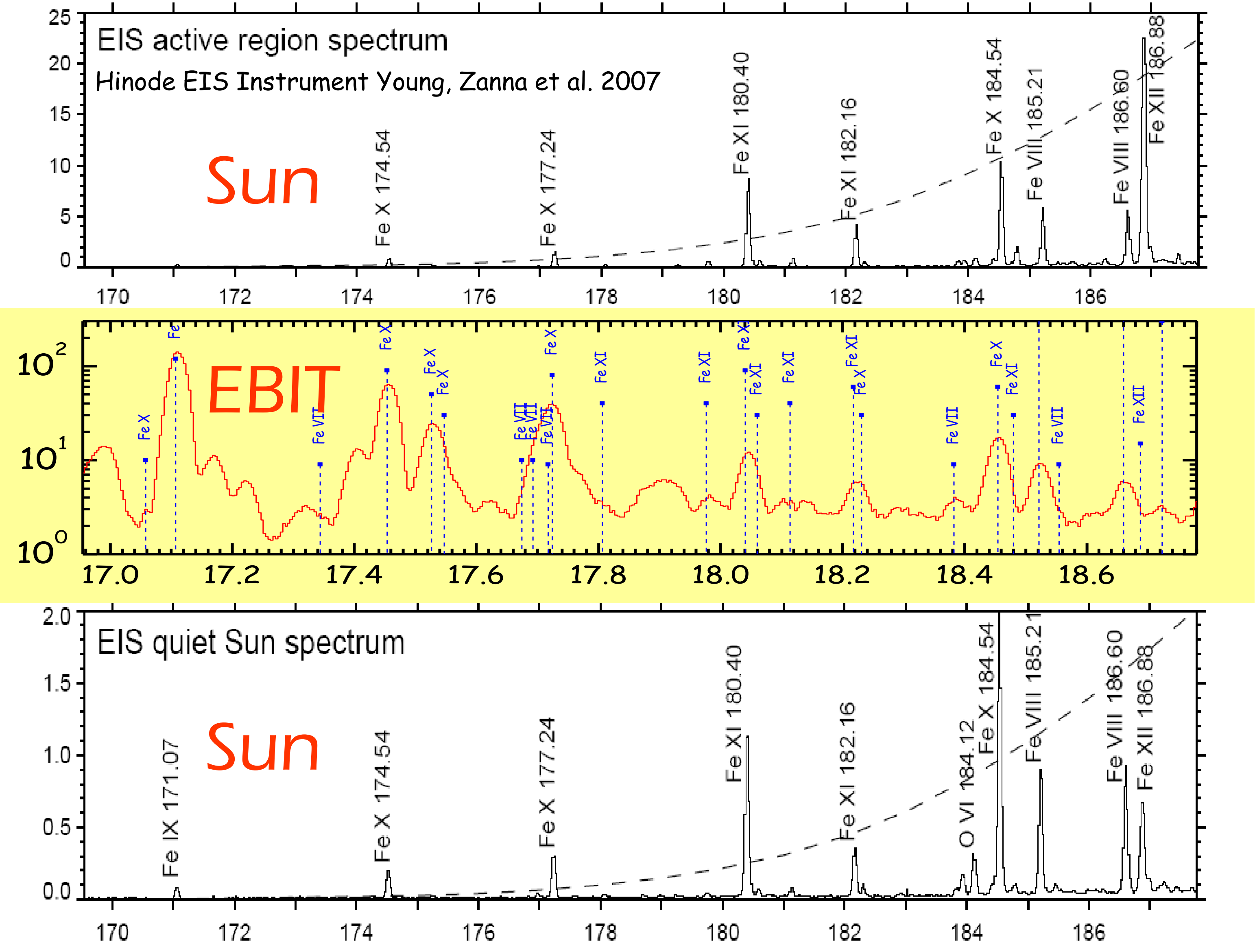

Hinode ("sunrise") is a solar space telescope mission launched in 2006 (Japan with US and UK partners) aiming at investigating the Sun's corona

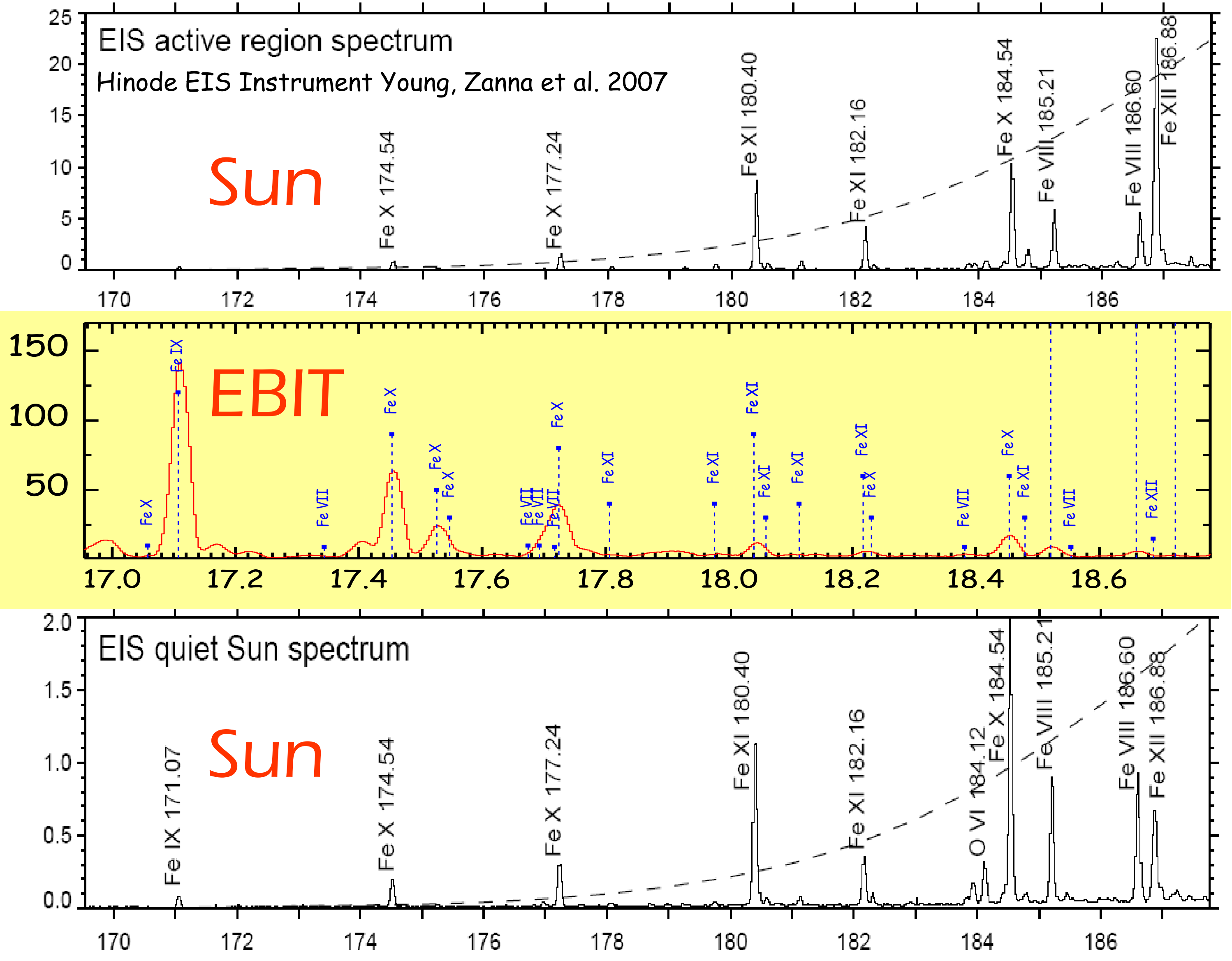

Reproducibility and error bars in the XUV

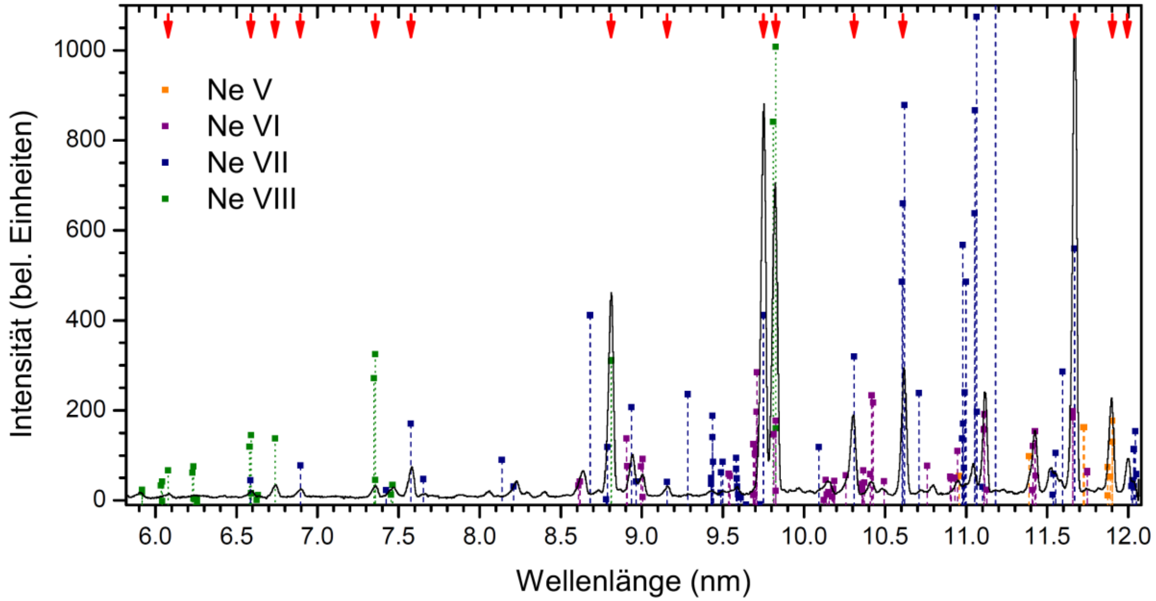

Ion	Wellenlänge	Position (Pixel)	Gesamtfehler
Ne VI	11,992 nm	2059,2(2)	0,005 nm
Ne V	11,901 nm	2029,12(9)	0,005 nm
Ne VII	11,669 nm	1963,4(1)	0,005 nm
Ne VII	10,61 nm	1649,76(1)	0,005 nm
Ne VIII	10,31 nm	1553,58(9)	0,005 nm
Ne VIII	9,826 nm	1403,58(8)	0,005 nm
Ne VIII	9,75 nm	1381,29(7)	0,005 nm
Ne VII	9,156 nm	1190,9(2)	0,005 nm
Ne VIII	8,809 nm	1077,63(7)	0,005 nm
Ne VII	7,577 nm	1657,9(1)	0,005 nm
Ne VIII	7,356 nm	578,6(2)	0,005 nm
Ne VII	6,89 nm	412,44(2)	0,005 nm
Ne VIII	6,738 nm	355,4(2)	0,005 nm
Ne VIII	6,589 nm	300,4(2)	0,005 nm
Ne VIII	6,079 nm	104,6(5)	0,005 nm

Reproducibility and error bars in the XUV

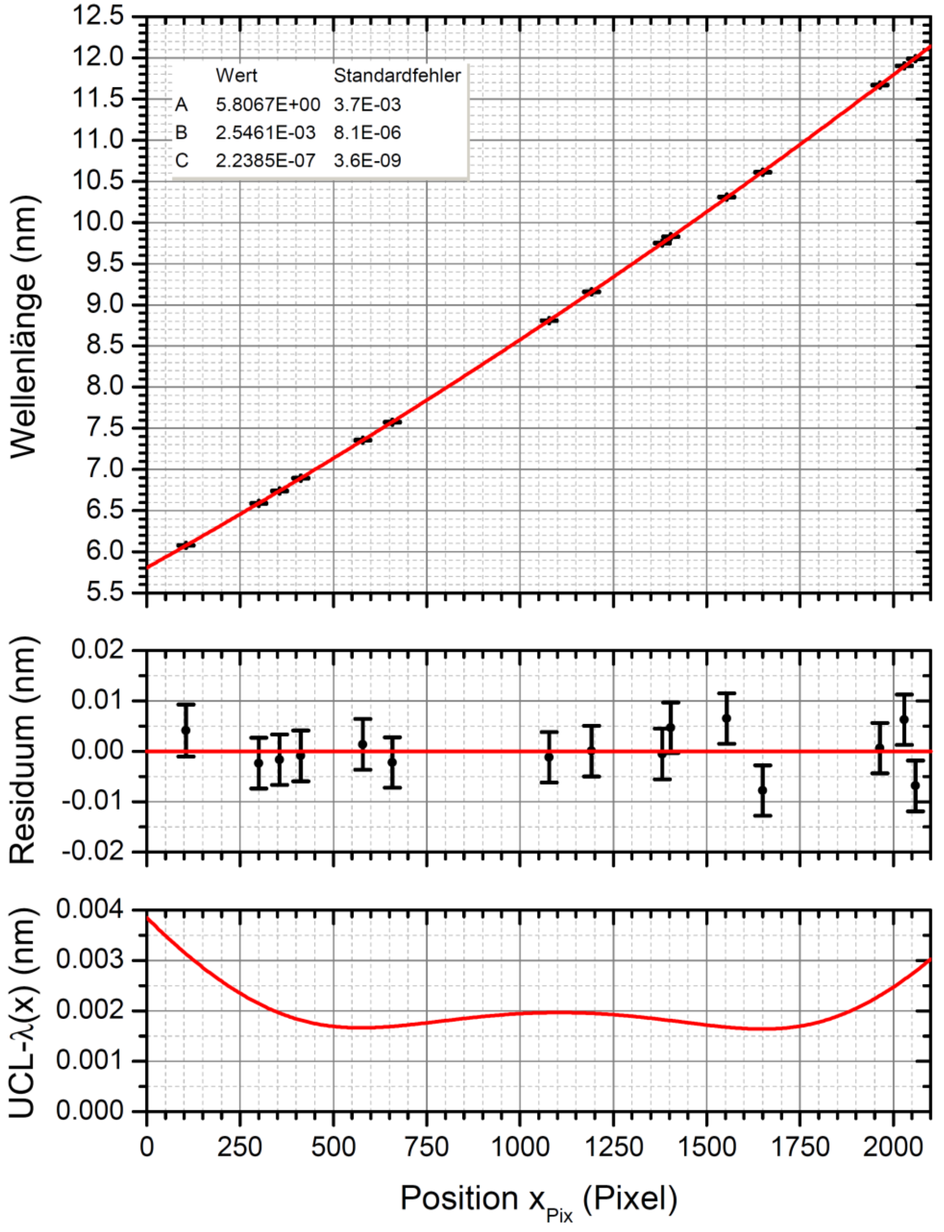

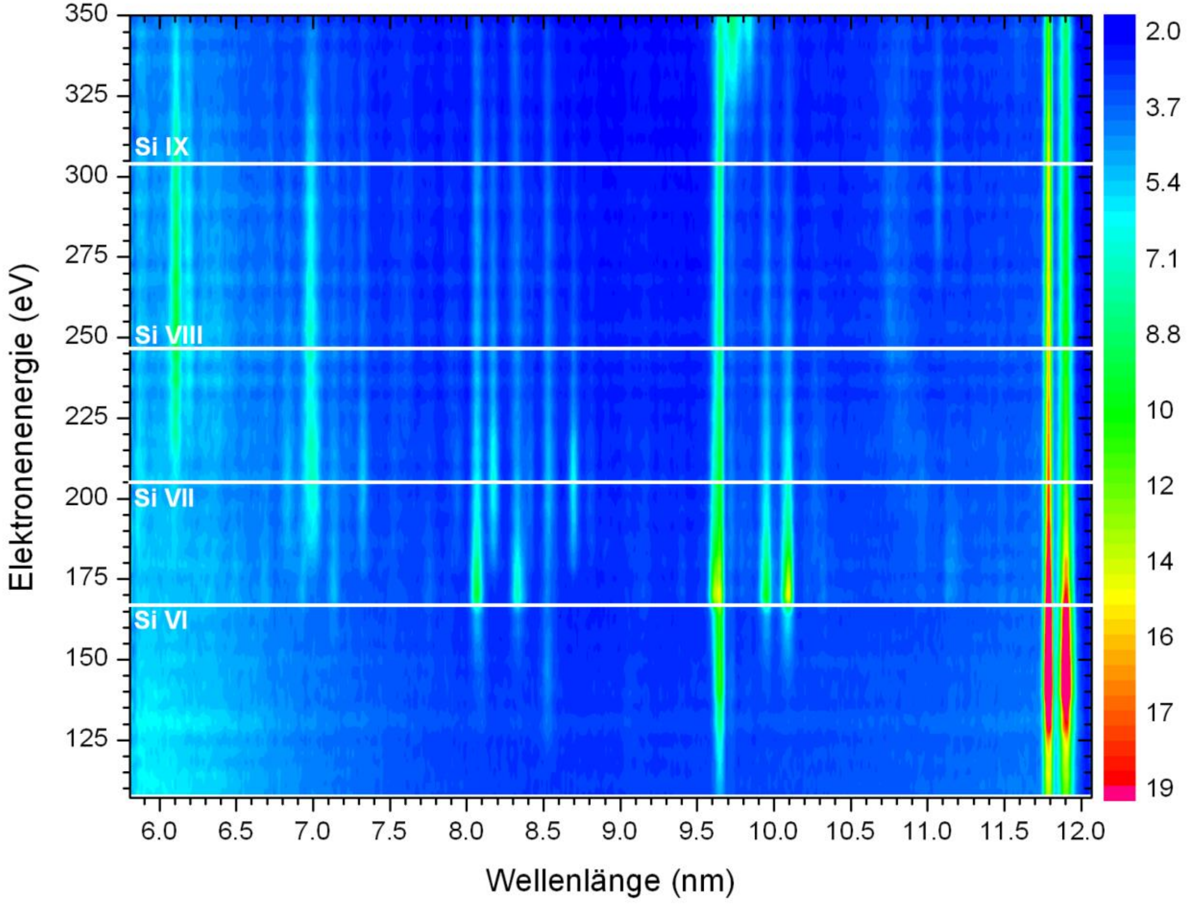

Ion	Übergang	**Diese Arbeit** λ (nm)	**[185]** λ (nm)	**[186]** λ (nm)
Si VIII	$3d\,^2F_{5/2} \to 2p^3\,^4S_{3/2}$	6,106(3)		6,1032
Si VIII	$3d\,^2F_{7/2} \to 2p^3\,^2D_{5/2}$	6,195(3)		6,1792
Si VI		6,490(3)		
Si VI	$5d\,^2D_{5/2} \to 2p^5\,^2P_{3/2}$	6,68(3)		6,6772 (NIST)
Si VII	$3d\,^5D_3 \to 2p^4\,^3P_1$	6,835(2)		6,8148
Si VI		6,932(2)		
Si VII	$3d\,^3F_2 \to 2p^4\,^3P_2$	6,990(2)		6,9664
Si VII	$3d\,^3F_3 \to 2p^4\,^1D_2$	7,014(2)		7,0072
Si VII	$3d\,^3G_3 \to 2p^4\,^1D_2$	7,136(2)		7,1384
Si VII	$3d \to 2p^4$	7,324(2)		7,312
Si VI	$3d \to 2p^5$	7,759(2)		7,7429 / 7,7718
Si V	$5d\,^1P^o_1 \to 2p^6\,^1S_0$	8,055(2)	8,054(2)	
Si VI	$3d \to 2p^5$	8,067(2)		8,0449 / 8,0725
Si V	$5d\,^3D^o_1 \to 2p^6\,^1S_0$	8,098(2)	8,078(1)	
Si VII	$3s \to 2p^4$	8,174(2)		8,1617 / 8,1845
Si VI	$3d\,^2D_{5/2} \to 2p^5\,^2P_{3/2}$	8,328(2)		8,3128
Si VI	$3d\,^2D_{3/2} \to 2p^5\,^2P_{1/2}$	8,378(2)		8,3611
Si VII	$3s\,1D_2 \to 2p^4\,^1D_2$	8,410(2)		8,4082
Si V	$4d\,^1P^o_1 \to 2p^6\,^1S_0$	8,526(2)	8,5177(8)	
Si V	$4d\,^3D^o_1 \to 2p^6\,^1S_0$	8,57(2)	8,558(1)	
Si VII		8,697(2)		
Si VII	$3s\,^3P_2 \to 2p^5\,^3P_2$	8,805(2)		8,8008
Si VI		9,618(2)		
Si V	$3d\,^1P^o_1 \to 2p^6\,^1S_0$	9,646(2)	9,6438(7)	
Si V	$3d\,^3D^o_1 \to 2p^6\,^1S_0$	9,726(2)	9,715(2)	
Si V	$3d\,^3P^o_1 \to 2p^6\,^1S_0$	9,830(5)		
Si VI		9,952(2)		
Si VI		10,092(2)		
Si V	$3s\,^1P^o_1 \to 2p^6\,^1S_0$	11,789(2)	11,7846(6)	
Si V	$3s\,^3P^o_0 \to 2p^6\,^1S_0$	11,873(2)		
Si V	$3s\,^3P^o_1 \to 2p^6\,^1S_0$	11,903(3)	11,8950(7)	
Si V	$3s\,^3P^o_2 \to 2p^6\,^1S_0$	11,938(3)	11,907(9)	

Tabelle 4.2: *Es sind die Pixelpositionen der Linien, ihre Fehler ΔPixel, die au. der NIST Datenbank [17] korrespondierenden Wellenlängen λ und deren Fehle: Δλ, sowie der Ladungszustand in der Tabelle eingetragen.*

Pixel	ΔPixel	λ (nm)	Δλ (nm)	Ladungszustand
43,539	0,029	17,453	0,007	Fe^{9+}
61,765	0,107	17,527	0,007	Fe^{9+}
108,380	0,058	17,724	0,007	Fe^{9+}
336,169	0,035	18,688	0,007	Fe^{11+}
368,306	0,031	18,822	0,007	Fe^{10+}
455,160	0,080	19,203	0,007	Fe^{23+}
464,759	0,399	19,239	0,007	Fe^{11+}
490,284	0,079	19,351	0,007	Fe^{11+}
527,308	0,030	19,512	0,007	Fe^{11+}
724,813	0,083	20,383	0,007	Fe^{12+}
1064,434	0,155	21,914	0,007	Fe^{13+}
1760,207	0,195	25,195	0,007	Fe^{12+}
1824,212	0,202	25,511	0,007	Fe^{23+}
1870,544	0,116	25,726	0,007	Fe^{9+}
2021,824	0,221	26,479	0,007	Fe^{13+}

Julia Jäger

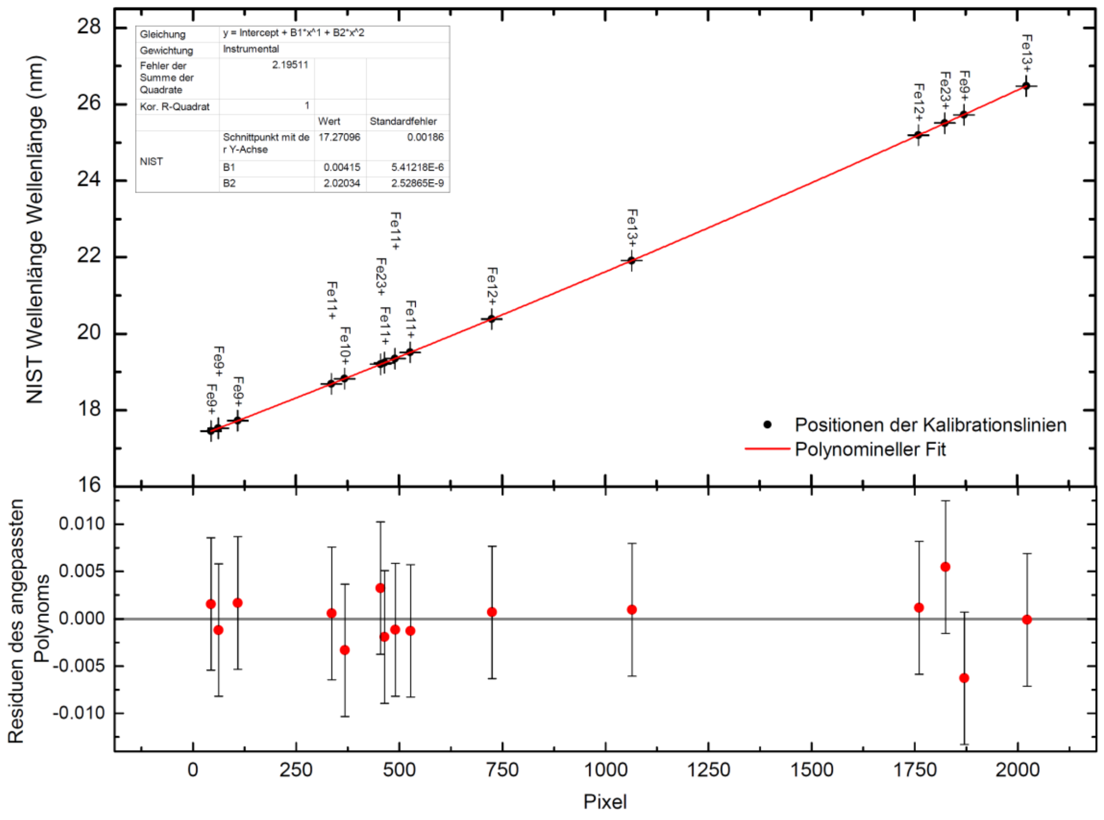

Julia Jäger

Longitudinal cut through the FLASH-EBIT

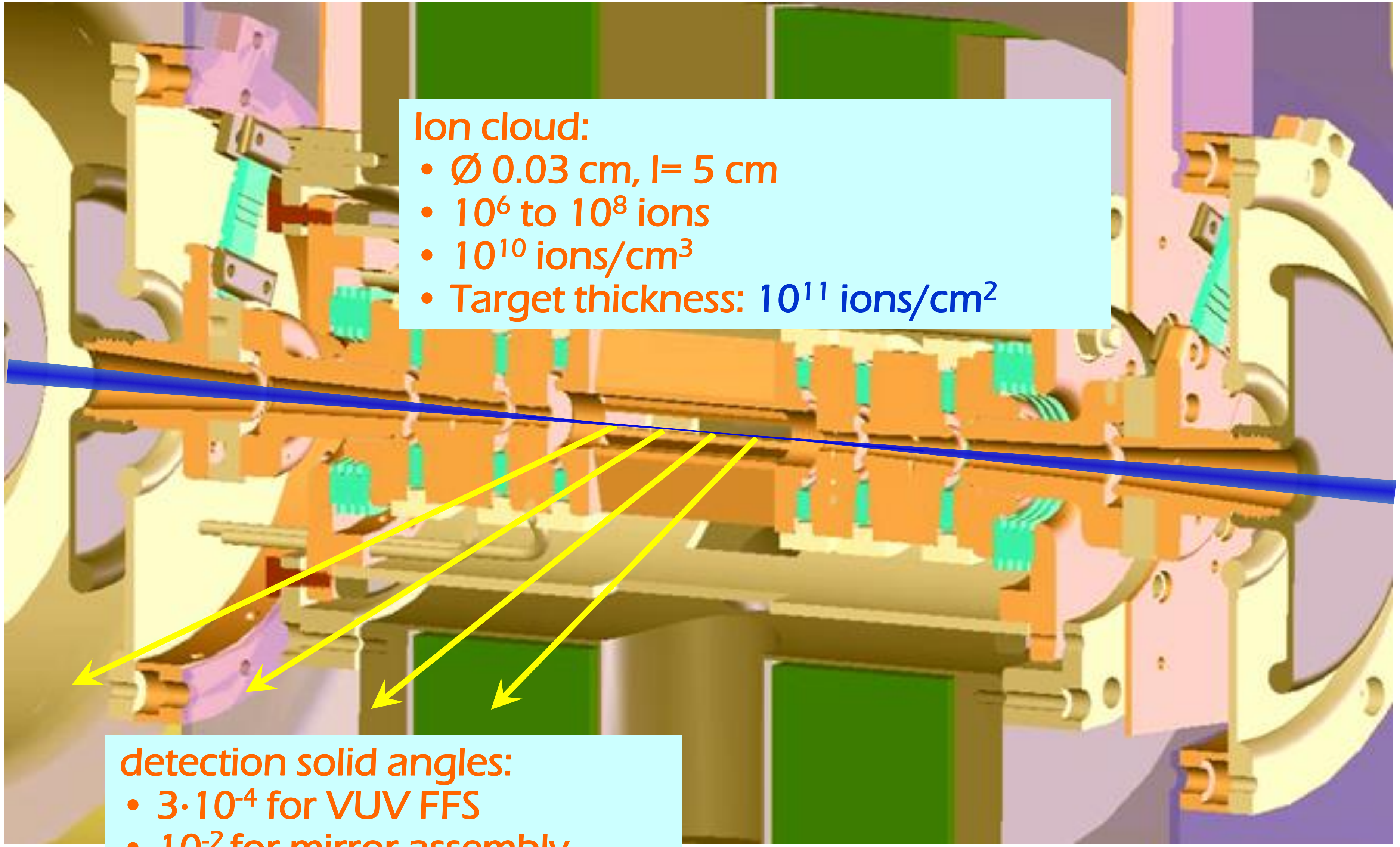

Ion cloud:

- Ø 0.03 cm, l= 5 cm
- 10^6 to 10^8 ions
- 10^{10} ions/cm^3
- Target thickness: 10^{11} ions/cm^2

detection solid angles:

- $3 \cdot 10^{-4}$ for VUV FFS
- 10^{-2} for mirror assembly

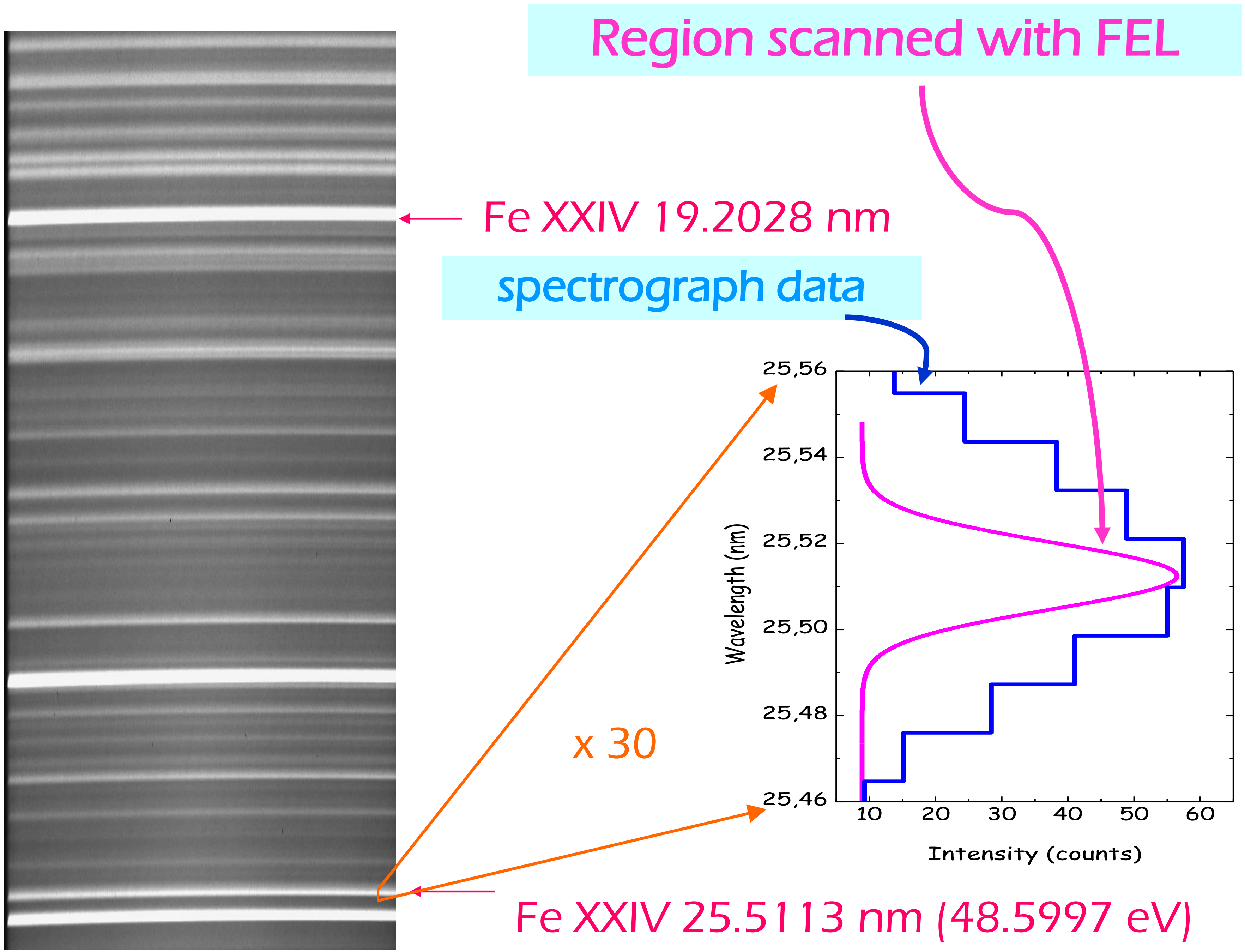

Region scanned with FEL
Fe XXIV 19.2028 nm
spectrograph data
x 30
25,56
25,54
25,52
25,50
25,48
25,46
Wavelength (nm)
10
20
30
40
50
60
Intensity (counts)
Fe XXIV 25.5113 nm (48.5997 eV)

ng spectrometer results

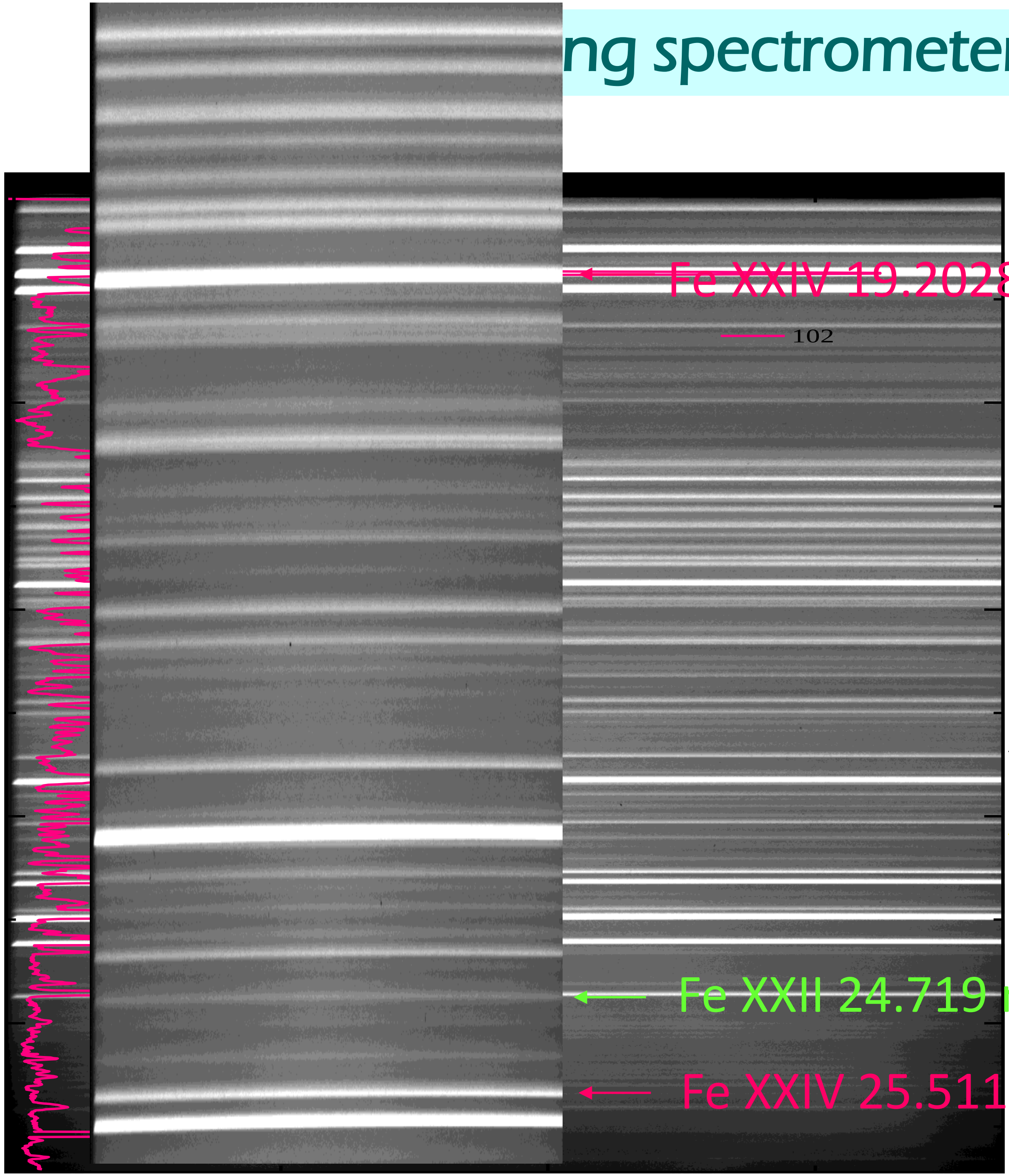

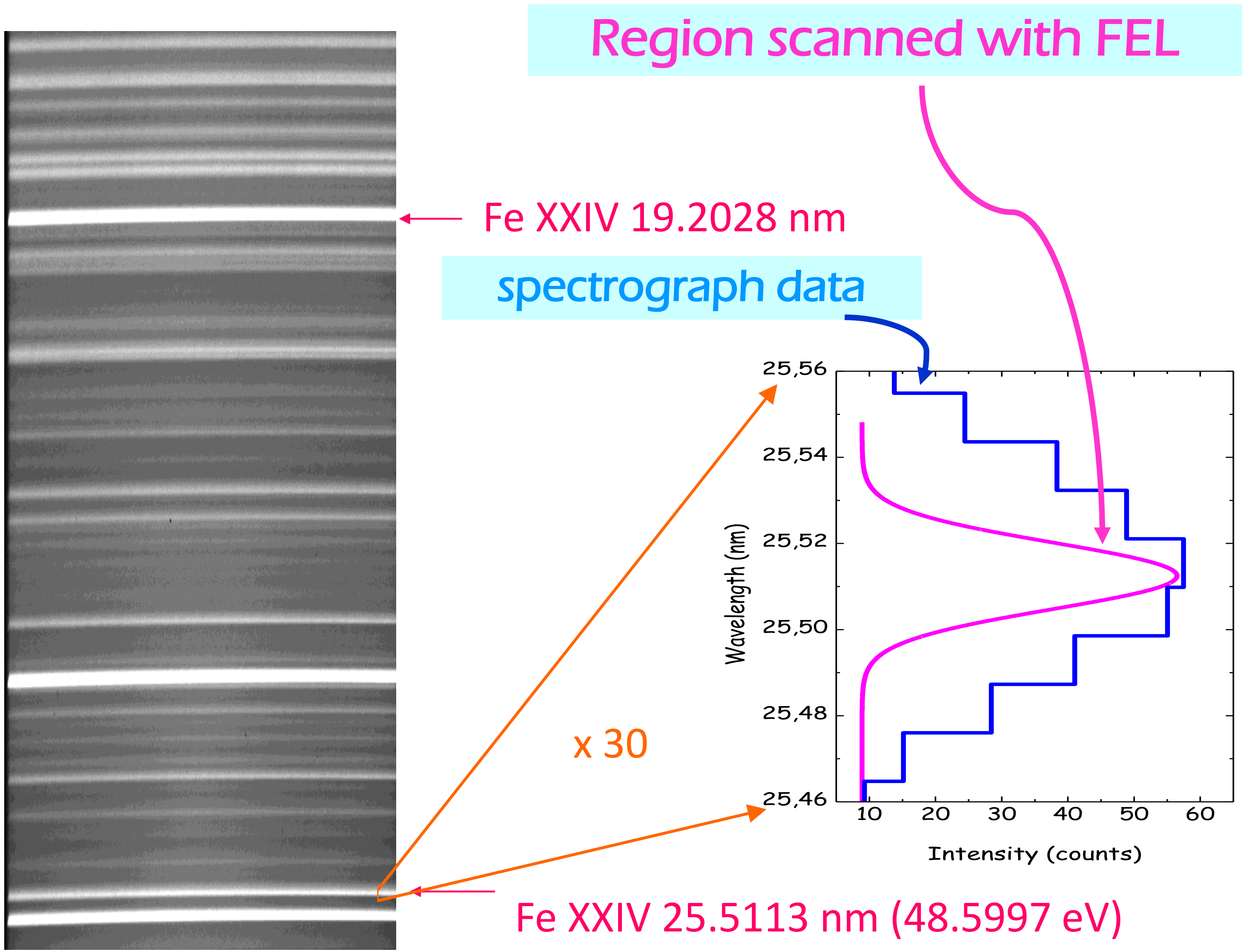

Region scanned with FEL
Fe XXIV 19.2028 nm
spectrograph data
25,56
25,54
25,52
25,50
25,48
25,46
Wavelength (nm)
x 30
10
20
30
40
50
60
Intensity (counts)
Fe XXIV 25.5113 nm (48.5997 eV)

Pm-like (61electrons) isoelectronic sequence

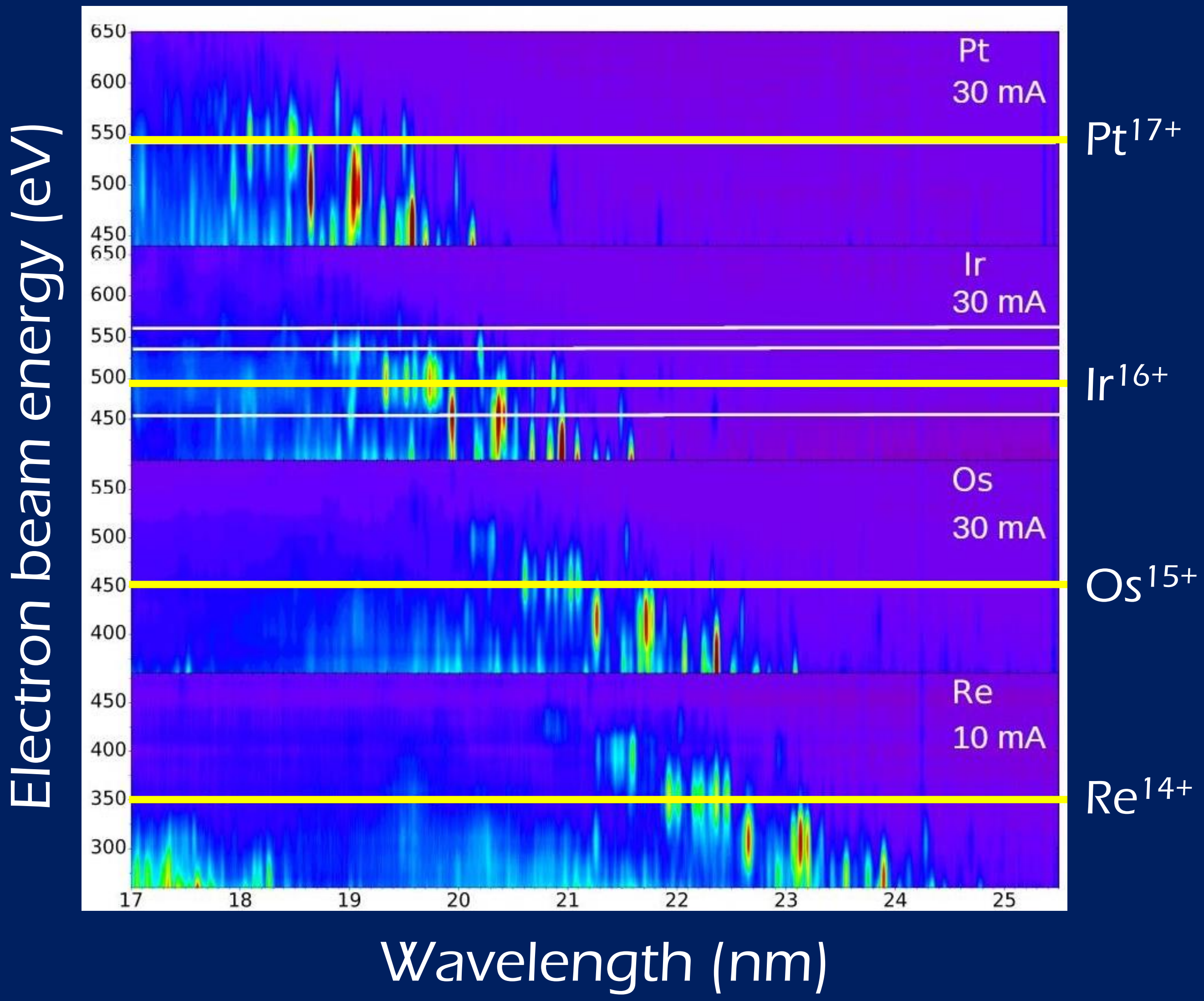

Ce (Z=58)
Pr (Z=59)
Nd (Z=60)
Pm (Z=61)
Sm (Z=62)

Isoelectronic sequence studied in detail to find analogies

Studies of Fe HCI with charge-state resolution

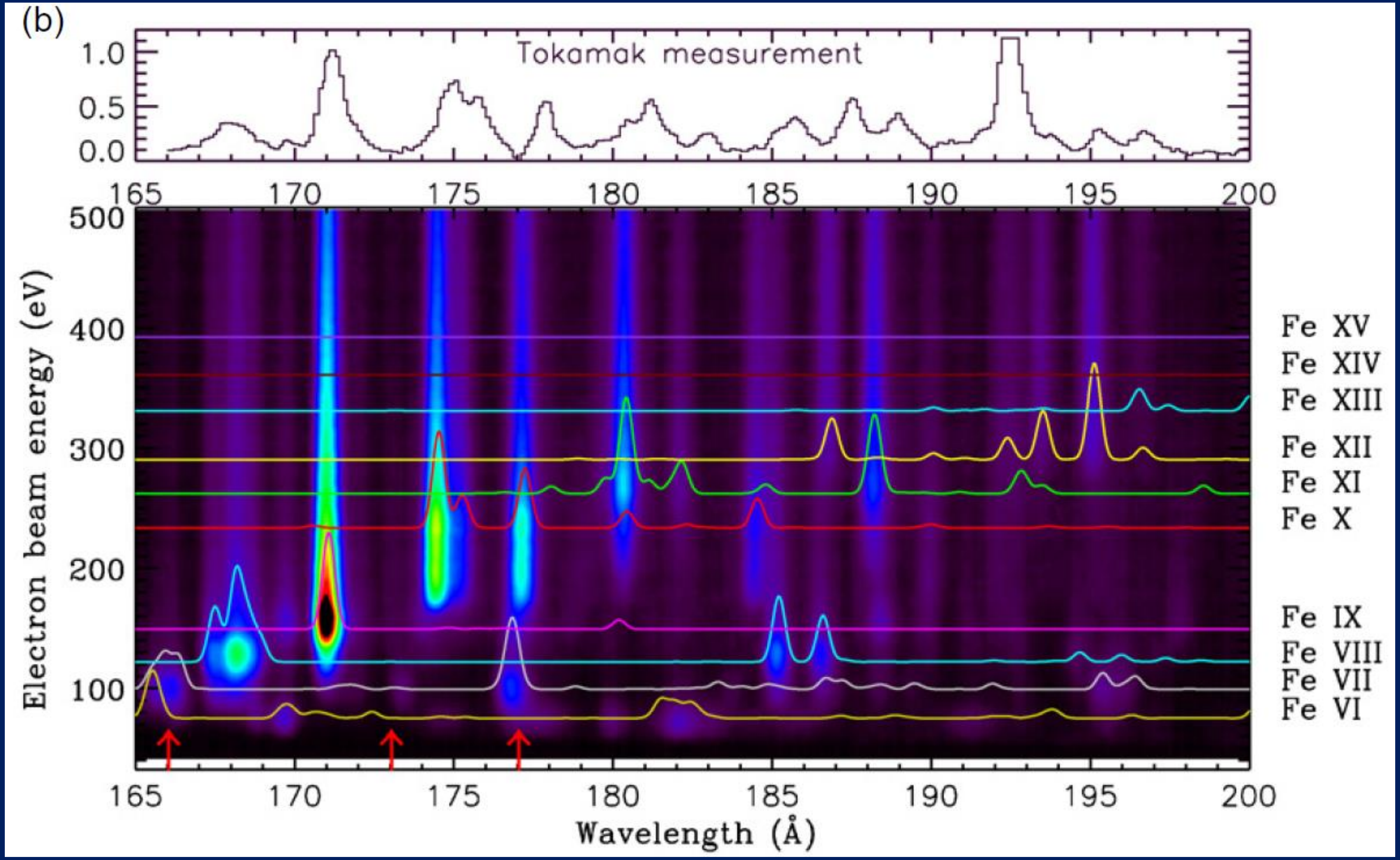

Gu et al., Astrophys. J. 696, 2275 (2009)

MAX-PLANCK-INSTITUT FÜR KERNPHYSIK

Understanding optical and EUV spectra of Sn ions

Understanding Sn spectra

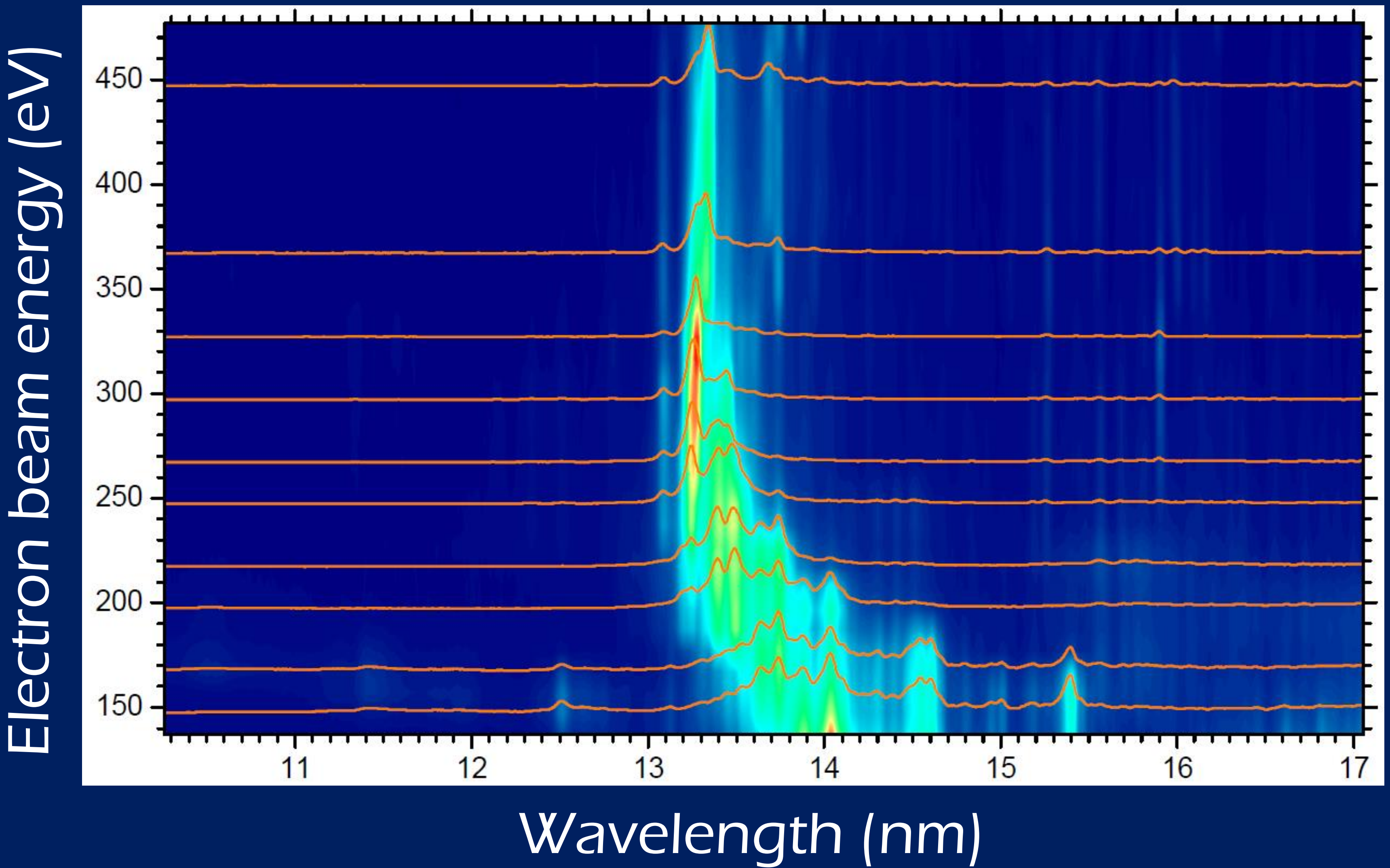

H. Bekker et al., J. Phys. B **48**, 144018 (2015)

Understanding Sn spectra

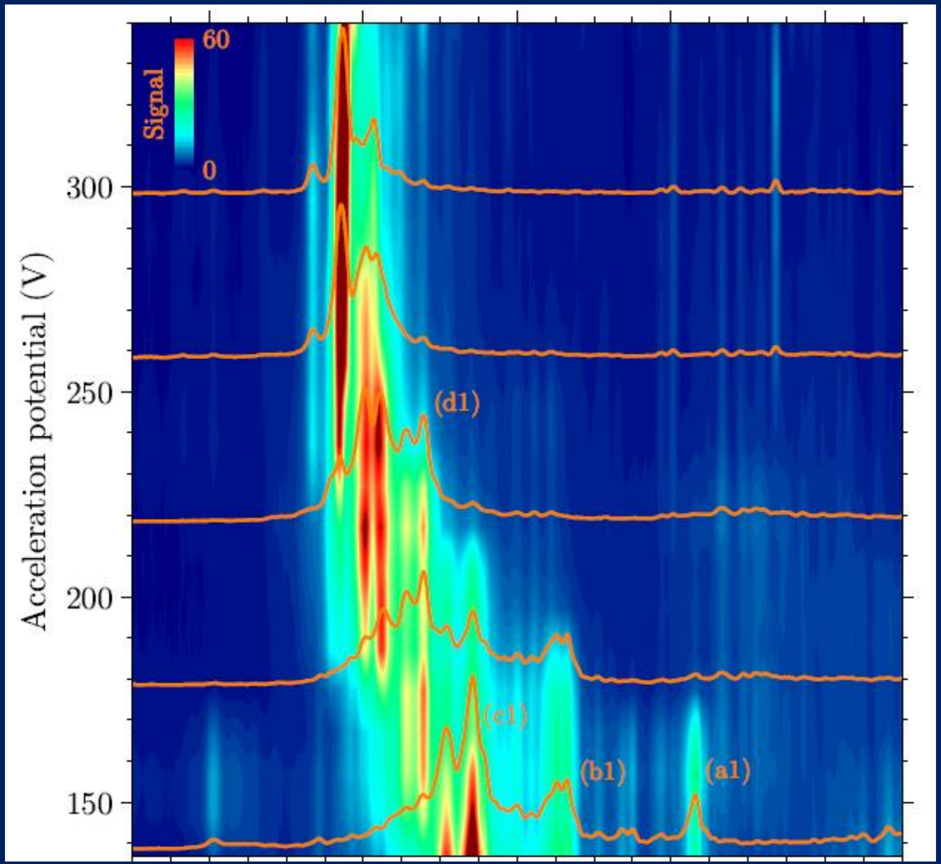

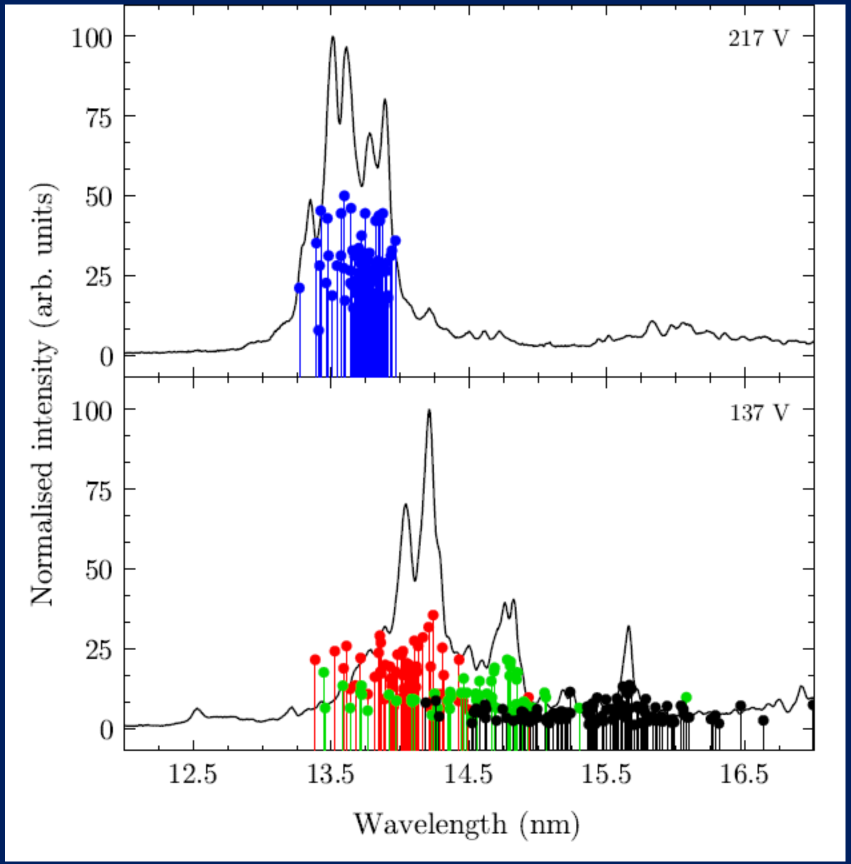

F. Torretti, ARCNL, PRA (2017)

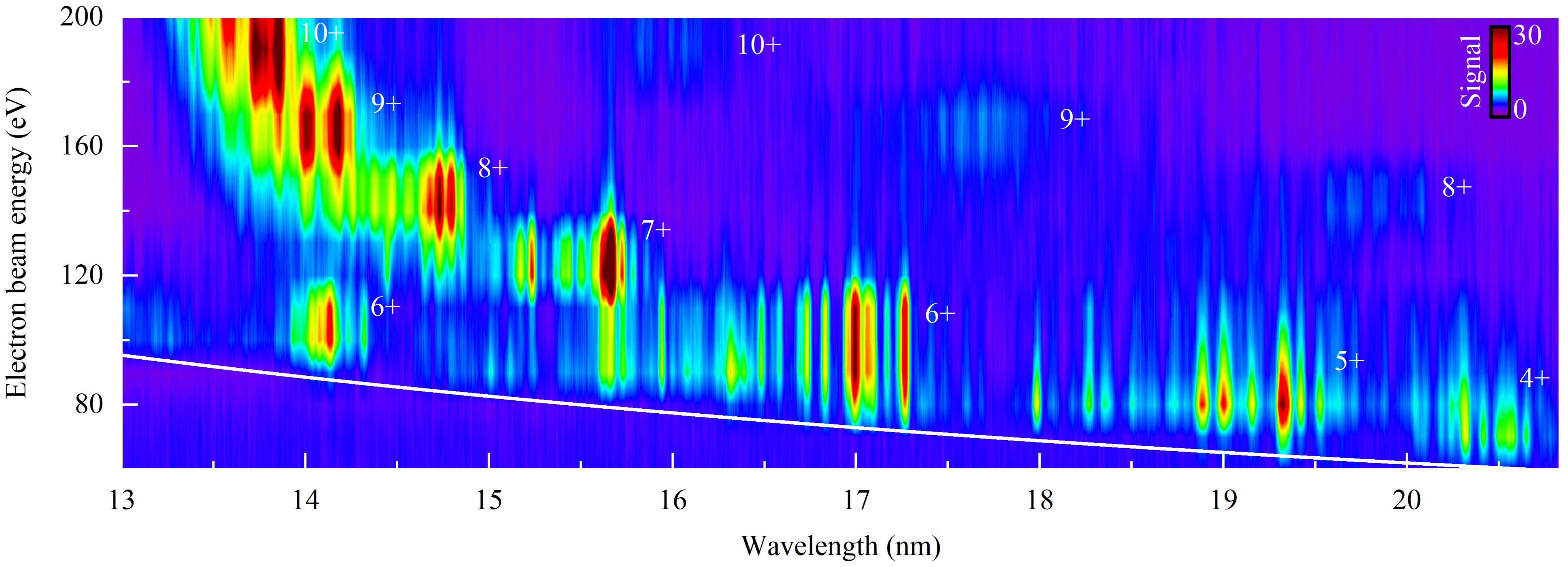

200
160
120
80
Electron beam energy (eV)
13
14
15
16
17
18
19
20
Wavelength (nm)
10+
9+
8+
7+
6+
5+
4+
Signal
30
0